Tu-Pos558

L-*CIS*-DILTIAZEM BLOCKS THE LIGHT-DEPENDENT K CONDUCTANCE OF *PECTEN* HYPERPOLARIZING PHOTORECEPTORS. ((Maria del Pilar Gomez and Enrico Nasi)) Department of Physiology Boston University School of Medicine and Marine Biological Laboratory Woods Hole, MA. (Spon. by M.C. Cornwall)

Hyperpolarizing photoreceptors in the distal retina of the scallop resemble vertebrate rods, not only structurally (the light transducing structure derives from modified cilia), but also functionally: the photocurrent is activated by cGMP and rectifies outwardly because of a voltage-dependent block by divalent cations. Because these light-dependent channels are K-selective and susceptible to block by 4-AP and TEA, they may represent a link between cyclic-nucleotide-gated channels and voltage-gated K channels; a kinship between these two families has been suggested on the basis of aminoacid sequence similarity. To further document the functional similarities between these channels and those of vertebrate photoreceptors, we examined the effects of l-*cis*-diltiazem, the best known antagonist of the light-sensitive conductance in rods. Local extracellular application of l-*cis*-diltiazem produced a swift, rapidly reversible suppression of the photocurrent. The $K_{1/2}$ was ≈450 μM, comparable to that obtained in rods under similar conditions. Intracellular dialysis of lower doses (100 μM) also induced a substantial inhibition. No change in the kinetics or the intensity-response relation of the photocurrent was induced by the drug, indicating that the inhibition results from block of the conductance, rather than impairment of the activating cascade; also, no use-dependence was observed, so that the site of action may not require opening of the channel. The blockage was voltage-dependent, increasing with membrane depolarization regardless of the side of application of the drug. On the assumption that the charged form l-*cis*-diltiazem$^+$ is active, this may suggest that the drug interacts with a site accessible from the intracellular compartment only. Supported by NIH grant RO1 EY-07559.

Tu-Pos559

A SLOW CURRENT INDUCED BY LIGHT IN RHABDOMERIC PHOTORECEPTORS: POSSIBLE RELATION TO I_{CRAC}. ((Maria del Pilar Gomez and Enrico Nasi)) Department of Physiology Boston University School of Medicine and Marine Biological Laboratory Woods Hole MA

In rhabdomeric photoreceptors PLC activation and formation of IP_3 are critical early events in phototransduction, and large Ca transients accompany the light response. In several species, Ca permeation through light-dependent channels is minute, and the increase in cytosolic Ca reflects chiefly internal release; repetitive stimulation in Ca-free media can lead to depletion of Ca stores and exhaustion of the photoresponse. In many cells that utilize the IP_3 signalling pathway, the ability to generate sustained responses and to replenish intracellular stores is mediated by a receptor-operated Ca influx mechanism (I_{crac}). In *Lima* rhabdomeric photoreceptors a slow after-depolarization follows intense light stimulation. Under voltage clamp, a corresponding inward current (I_{slow}) can be reproducibly measured; this current develops with a latency of 5-10 s, reaches a peak amplitude ≈100-200 pA in 30-40 s, and decays in 1-3 minutes. I_{slow} is graded with light intensity, but is wavelength-insensitive, which, together with the sluggish activation, rules out a PDA phenomenon. I_{slow} obtains after replacing Na_o with Li, guanidinium, or NMDG, indicating that it is not due to an electrogenic Na/Ca exchange mechanism. Its reversal potential in normal ionic conditions is ≈+30 mV. I_{slow} can be evoked with extracellular Ca (60 mM) as the sole permeant species; Ba can substitute for Ca but Mg cannot. This slow current resembles I_{crac} described in other cells after IP_3 stimulation, and may play an important role in the homeostasis of the Ca stores implicated in the generation of the photoresponse. Supported by NIH grant EY07559

Tu-Pos560

TYROSINE KINASE ACTIVITY IN RETINAL ROD OUTER SEGMENT MEMBRANES. POSSIBLE RELATION TO PHOSPHOINOSITIDE METABOLISM AND ROD FUNCTIONING. ((I.D. Volotovski, A.M. Sholuh, I.D. Artamonov*, L.A. Baranova)) Institute of Photobiology, Academy of Sciences of Belarus, Minsk 220073, Belarus; *Shemjakin-Ovchinnikov Institute of Bioorganic Chemistry, Russian Academy of Sciences, Moscow 117871, Russia.

Protein tyrosine kinases (PTK) are involved in the regulation of many cellular programs and are responsible for the phosphorylation of various cytoplasmic substrates including phospholipases of γ-family. to propagate a ligand-mediated receptor protein tyrosinase signal via the substrates into the cellular responses. Up to now, no information was obtained on the existence of PTK in vertebrate retinal rods. Using two approaches, it was shown that outer segments of bovine rods (ROS) contain tyrosine kinase activity associated with the disc and plasma membranes. A protein product to be phosphorylated had a molecular mass in the range of 70 kDa. Besides, poly(Glu-Tyr) 4:1, the artificial substrate for tyrosine kinases was markedly phosphorylated when it was added to retinal membrane suspension. The influence of light, ion composition and G-protein on tyrosine kinase activity in ROS was studied. The possible relation of tyrosine kinase-activated phosphorylation with phosphoinositide metabolism in rod outer segment was discussed.

TRANSPORTERS AND CHANNELS: FUNCTIONAL SIMILARITIES

W-AM-SymI-1

STRUCTURE AND FUNCTION OF MOLECULAR WATER CHANNELS. ((A.S. Verkman)) Cardiovascular Research Institute. University of California, San Francisco, CA 94143-0521.

Remarkable progress has been made recently in the identification and characterization of water transporting proteins ("water channels", "aquaporins"). There are at present 5 water channels in mammals, >30 from plants and several from amphibia and bacteria. The water channels are small hydrophobic proteins with sequence homology to MIP; in mammals, the water channels are expressed widely in plasma membranes of epithelial and non-epithelial tissues. The majority of molecular-level information about water transporting mechanisms comes from studies on CHIP28 (AQP1), a 28 kDa glycoprotein that forms tetramers in membranes; recent electron cryo-crystallographic data suggests that each monomer contains 6 helical domains surrounding a central aqueous pathway. Functional analysis shows that CHIP28 monomers function independently as water-selective channels without transporting protons, ions or small solutes. Only mutations in the vasopressin-sensitive water channel (AQP2) have been shown to cause human disease - non-X-linked congenital, nephrogenic diabetes insipidus; the physiological significance of other water channels remains unproven. One mercurial-insensitive water channel has been identified (MIWC, AQP4), which has the unique feature of multiple overlapping transcriptional units. Another homolog transports glycerol > water (GLIP, AQP3). Water channels have been expressed in *Xenopus* oocytes, mammalian and insect cells, and yeast. Major questions in the field are the role of water channels in normal physiology and disease, the existence of water channel regulatory mechanisms, and the determination of structure at atomic resolution.

W-AM-SymI-2

MECHANISM OF MULTIDRUG TRANSPORT.((M. Gottesman)) National Cancer Institute.

W-AM-SymI-3

MICROSECOND TIME SCALE MEASUREMENTS OF SODIUM TRANSPORT.
((D.W. Hilgemann)), Dept. of Physiol, UTSW, Dallas, TX, 75235

Partial transport reactions of a sodium-coupled ion pump (the Na,K ATPase), a sodium-coupled exchanger (the cardiac NCX1 Na,Ca exchanger) and a sodium-coupled cotransporter (the GAT1 Na,Cl,GABA cotransporter) have been studied at microsecond resolution in giant membrane patches. The question is asked, to what extent molecular mechanisms underlying the transporter signals are comparable to (or not comparable to) molecular mechanisms in channel function. 1) Fast (<3μs) charge movements have been associated with extracellular sodium binding in Na,K pump and NCX1. *Possible analogy: Binding of blocking ions to open channels (or permeant ions to closed channels).* 2) Opening of Na,K pump to the extracellular side is nearly voltage-independent. *Possible analogy: Final (voltage-independent) step of channel opening.* 3) Fast (40μs) charge movements which occur in the empty GAT1 transporter are suppressed by ion binding. *Possible analogy: Flexing of ion-coordinating groups in open channels.* 4) A significant noise of Na,Ca exchange current in small patches evidently arises from exchanger gating by an inactivation process and defines unitary exchanger currents of ap.1 fA. *Possible analogy: Channel gating.*

W-AM-SymI-4

NEUROTRANSMITTER TRANSPORTERS: GATING AND PERMEATION PROPERTIES
(H. A. Lester) Caltech, Pasadena CA 91125

Plasma membrane neurotransmitter transporters are important for neuroscience and for medicine. One family comprises ~ 4 transporters for glutamate; another comprises ~ 12 transporters for other known neurotransmitters. "Electrogenicity" is a concept previously thought to explain currents that arise from fixed stoichiometry of ion coupling during symport and antiport. But now functional properties of these molecules can be tested with high resolution in heterologous expression systems; and many additional electrophysiological properties have been described as follows. Leakage currents occur in the absence of neurotransmitter. Charge movements are associated with individual steps in the transport cycle and are measured by voltage-jump and concentration-jump relaxations. There is variable stoichiometry; for instance, Na^+ and Cl^- currents flow through serotonin and glutamate transporters in excess amounts, and even in inappropriate directions, during substrate flux. There are even unitary currents that resemble single- channel records. Site-directed mutagenesis, which has proven successful in the channel world, may soon help to define the permeation pathway. Simulations and models for neurotransmitter transporters have previously been based on traditional alternating-access models; but more recent simulations also emphasize the similarity with single-file transport in a channel-like lumen.

K CHANNELS - INWARD RECTIFIERS

W-AM-A1

ALTERING THREE AMINO ACIDS CONVERTS AN OUTWARD RECTIFYING POTASSIUM CHANNEL INTO AN INWARD RECTIFYING POTASSIUM CHANNEL.
((A.G. Miller and R.W. Aldrich)) Dept. of Mol. and Cell. Phys., HHMI, Stanford Univ., Stanford Ca. 94305.

In order to explain the sequence similarities between a plant inward rectifying potassium channel (KAT1) and the family of outward rectifying potassium channels we attempted to convert the *Shaker B* channel into an inward rectifier. Single, double, and triple point mutations in the S4 segment of the ShB channel progressively shift the activation properties of ShB to hyperpolarized voltages, resulting in a greater number of channels in the inactivated state at hyperpolarized voltages. In high external potassium, hyperpolarization from -80 mV of the triple point mutant results in recovery from inactivation through the open state, and a large inward current. Depolarization from -80 mV of this channel results in further inactivation and a decay in the outward current. A steady state I-V curve for the triple mutant shows inward rectification, similar to the steady state I-V curve for KAT1. What is traditionally considered activation of an inward rectifier is, in the case of the triple point mutant, recovery from inactivation. Similarly, what is usually considered deactivation is inactivation. Deleting a 41 amino acid segment from the N-terminal of ShB channels with the same single, double, and triple point mutations shows that the progressive steady state inward rectification resulting from the hyperpolarizing shift in activation is related to the presence of N-type inactivation. A three state scheme with one activation gate and one inactivation gate is sufficient to explain the gradual change from an outward rectifier to an inward rectifier. Since only three amino acids have been changed these results suggest a structural conservation between outward rectifying and inward rectifying channels, and could be used to support similar conclusions regarding the HERG channel which has inward rectifying properties and is a member of the eag family of outward rectifiers.

W-AM-A2

INVOLVEMENT OF THE C- AND N-TERMINUS IN REGULATION OF THE INWARD RECTIFIER KAT1.
((I. Marten and T. Hoshi)) Dept. of Physiology and Biophysics, The University of Iowa, Iowa City, IA 52242.

The potassium channel KAT1 shares a high similarity in sequence with the K^+ channels of the *eag* family. However, KAT1 currents can be only recorded upon hyperpolarization and run down on membrane patch excision. The structural basis of those channel features were studied on wildtype and mutated KAT1-channels expressed in *Xenopus* oocytes.
In macro-patches, the run down of the wildtype channel was accompanied by a slow-down in activation and a faster deactivation resulting in a shift of the activation threshold potential towards more hyperpolarized potentials. We examined whether cytoskeletal elements are involved in KAT1 run-down. When KAT1-expressing *Xenopus* oocytes were treated with colchicine (100 µM), a microtubule disrupter, we observed a decrease in the macroscopic current. But colchicine affected neither the voltage dependence nor the activation or deactivation time course.
Since the run down is likely to be linked to the loss in interaction between the channel protein and cytoplasmic component(s), we deleted various parts of the intracellular C- and N-terminus. When the whole C- or N- terminal segment (Δ2-34; Δ311-677) was removed, macroscopic currents could not be detected. Smaller deletions of the C-terminus (e.g. Δ541-677) resulted in functional expression of KAT1. The gating characteristics and response to patch excision of the functional mutants were similar to those of the wildtype channel. The results indicate that N- and the C-terminus are important for the functional expression of KAT1.
(Supported by HFSP, NIH.)

W-AM-A3

MECHANISM OF INWARD RECTIFICATION IN THE HERG POTASSIUM CHANNEL
((Paula L. Smith, Thomas Baukrowitz and Gary Yellen)) Department of Neurobiology, Harvard Medical School and Massachusetts General Hospital, Boston, MA

Voltage-activated K channels in the heart provide the impetus for repolarization of the myocardial membrane potential and are thus an important determinant of the duration of the cardiac action potential. One particular K channel gene, HERG, has recently been shown to be linked to an inherited form of long QT syndrome, a disturbance of the cardiac rhythm that often leads to sudden cardiac death. This gene appears to code for the I(Kr) current, a member of the voltage-activated K channel superfamily with an unusual form of inward rectification.

Our experiments on heterologously expressed HERG channels reveal the mechanism of the inward rectification to be a rapid and voltage-dependent form of C-type inactivation, a gating mechanism often considered to be the "slow inactivation" mechanism of other K channels. Changing internal [Mg] or blocking with internal TEA produces no change in the kinetics of the rapid inactivation, arguing against inactivation by internal blockers or by an internal inactivation particle. By contrast, blockade by external TEA slows entry into the inactivated state, suggesting that inactivation involves the outer mouth of the channel (like the C-type inactivation of Shaker channels). Consistent with this idea, mutations in the outer part of the pore abolish the inactivation process.

W-AM-A4

MECHANISM OF HERG RECTIFICATION IS FAST INACTIVATION.
((P.S. Spector, M.E. Curran, A. Zou, M.T. Keating, M.C. Sanguinetti)) Cardiology Division, University of Utah, Salt Lake City, UT 84112.

HERG encodes a cardiac delayed rectifier K^+ channel, I_{Kr}. The I-V relationship of HERG has a negative slope conductance at potentials positive to ~ 0 mV. Rectification of HERG was not affected by exposure of the inside face of excised patches to a Mg^{2+}-free bath solution, indicating that fast inactivation is an intrinsic gating process, and not due to voltage-dependent block by Mg^{2+} and polyamines as reported for inward rectifier K channels. We used a dual pulse protocol to directly measure the onset of fast inactivation. Following a depolarizing pulse to +40 mV, the membrane was hyperpolarized briefly to permit recovery from inactivation but not deactivation. This pulse was immediately followed by a second depolarization to allow detection of reopened channels before the onset of inactivation. The magnitude of instantaneous currents measured during the second depolarization was a linear function of test potential. Truncation of the N-terminal region of HERG did not remove fast inactivation, but shifted the voltage-dependence of channel gating to more depolarized potentials, and increased the rate of deactivation (e.g., τ_{fast} = 278±43 ms vs 22±3 ms at -90 mV). The extent of HERG channel inactivation increases with membrane depolarization, and proceeds at a rate $\geq$ 10 times faster than the fast component of activation (e.g., τ = 9.8±0.2 ms vs 104±22 ms at 0 mV). This results in a progressive decrease in current amplitude as the membrane is depolarized above -20 mV.

W-AM-A5

SINGLE CHANNEL PROPERTIES OF HERG, THE CHANNEL ENCODING I_{Kr}.

((J. Kiehn, A. Lacerda, B. Wible, M. Sanguinetti*, M. Keating*, A.M. Brown,))
Rammelkamp Center for Research, Case Western Reserve University, Cleveland, OH.
* Univ. of Utah Health Sci. Center, Salt Lake City, UT 84112.

Recently it was demonstrated, that HERG expressed heterologously in Xenopus oocytes produces a current which has the macroscopic characteristics of I_{Kr}. (Sanguinetti et al 1995).

By using variance analysis of macropatch currents we calculated a single channel conductance of 2 pS at an extracellular potassium concentration of 5 mM and 9 pS at 100 mM.. Direct single channel measurements confirmed the value at 100 mM K^+. We made a detailed single channel analysis and calculated the single channel conductance to be 9.2 pS, the mean open time to be 3.2 ms and two closed times to be 0.6 and 22 ms at -100 mV membrane potential and 100 mM extracellular potassium. These values resemble the values found for I_{Kr} in cardiomyocytes isolated from guinea pig. HERG was also blocked by low concentrations of the Class III drug Dofetilide, which is known to block I_{Kr}.

These biophysical and pharmacological properties further support that HERG encodes I_{Kr} in cardiomyocytes. (supported by the "Deutsche Forschungsgemeinschaft" and NIH-grants HL-37044 and HL-36930).

W-AM-A6

UNUSUAL KINETIC AND ION TRANSFER PROPERTIES OF THE E-4031 SENSITIVE REPOLARIZATION CURRENT (I_{Kr}) IN RABBIT VENTRICULAR MYOCYTES.

((J.R. Clay*, A. Ogbaghebriel+#, T. Paquette+, B. Sasyniuk#, and A. Shrier+)) *NIH, Bethesda, MD 20892, Depts. of +Physiology and #Pharmacology, McGill Univ., Montreal, Quebec, Canada H3G 1Y6.

We have observed novel kinetic and ion-transfer properties of I_{Kr} in rabbit ventricular myocytes with the patch-clamp technique. The reversal potential, E_{rev}, for I_{Kr} is ~ 15 mV positive to E_K in physiological saline (Ogbaghebriel, Clay, & Shrier 1995, *Biophys. J.* 68:A37). Consequently, this channel passes *inward* current during the latter part of repolarization, although the effect is minimized by the rapid deactivation kinetics of I_{Kr} when the net current is inward (current-dependent gating). For example, I_{Kr} deactivation at -70 mV in 1 mM K_o (outward current) is ~ 200 ms, whereas it is ~ 5 ms at -70 mV with 5 mM K_o (inward current). Another unusual feature of this channel is that the midpoint of its activation curve is at ~ +10 mV on the voltage axis, as compared to -30 mV for the maximum time constant (~0.8 sec at T=33-34° C). Moreover, the width of the bell-shaped activation curve which describes the kinetics is much broader than the steepness of the activation curve would predict. These results comprise a gating paradox which cannot be resolved by the addition of a fast inactivation gate to the analysis. In summary, our results provide unusual constraints on the molecular mechanisms which underlie I_{Kr} gating. (Supported by MRC and FCAR, Canada.)

W-AM-A7

AN N-TERMINAL SITE CONTROLS DIFFERENTIAL BLOCKER-RELEASE IN K_{IR} 2.1 CHANNELS

((J. P. Ruppersberg, B. Fakler, U. Brändle, H.-P. Zenner and J. H. Schultz))
Dept. of Sensory Biophysics, ENT-Hospital of the University of Tübingen

Activation of inward currents in response to hyperpolarizing voltage pulses differs between various subtypes of the K_{ir} family. While ROMK1 ($K_{ir}1.1$) channels show instantaneous activation, this process is slow in GIRK1 ($K_{ir}3.1$) channels and intermediate in BIR10 ($K_{ir}4.1$), BIR11 ($K_{ir}2.3$) and IRK1 ($K_{ir}2.1$) channels. Since it is known that activation depends on release of intracellular blocking ions such as polyamines (spermine (SPM) and spermidine) and divalent cations (Mg^{2+}), we were interested in differential blocker-release between K_{ir} subtypes. Comparing blocker-release properties among various clones we realized that IRK1, as cloned in our laboratory, showed a slow Mg^{2+} release (10.2±0.4 ms at -50mV) associated with an intermediate spermine (SPM) release (1.6±0.3 ms at -50mV), while the corresponding clone published by Kubo et al. (1993, Nature 362:127) showed a fast release for SPM (0.3±0.1 ms) and Mg^{2+} (0.1±0.05 ms) Both IRK1 clones differed by only one residue located in the N-terminus: residue 84 is threonine in our clone, while it is methionine in the clone of Kubo et al. (T84M). The homologues residue in ROMK1 is lysine (K), while it is asparagine (N) in GIRK1. Mutation-analysis at residue 84 in IRK1 revealed fastest release of both, Mg^{2+} and SPM, for the T84K mutation (< 0.1 ms) and slowest release for the T84N mutation (48.5±1.5 ms and 24.2±0.5 ms). Heteromultimerisation between IRK1(84T) and IRK1(84M) revealed slow Mg^{2+} release, while removal of the negatively charged D at position 172 in IRK1(84T) resulted in fast Mg^{2+} unblocking (< 0.1 ms).

W-AM-A8

ABSENCE OF GLUCOSE-REGULATED K^+_{ATP} CURRENT IN PANCREATIC ß-CELLS OF PHHI.

((L.H. Philipson, J.F. Worley III, M.W. Roe, A. Mittal, A. Kuznetsov, N.T. Blair, K. Ghai, M.S. McIntyre, M.E. Lancaster, and I.D. Dukes))
Univ. of Chicago, Chicago, IL 60637 and Glaxo Res. Inst., Research Triangle Park, N.C. 27709.

Mutations in the human sulfonylurea receptor gene (SUR) have been linked to persistent hyperinsulinemia and hypoglycemia of infancy (PHHI). PHHI is associated with hyperplasia of pancreatic islets, but the membrane currents in the insulin-secreting ß-cells have not been well characterized. An infant with PHHI underwent pancreas resection; histopathologic examination revealed typical features of islet hyperplasia. Amplification of cDNA from PHHI islets showed SUR mRNA was present. Isolated PHHI islets and dispersed islet cells were cultured for intracellular calcium ($[Ca^{2+}]_i$), membrane potential and current measurements. In adult islets, glucose, tolbutamide and carbachol increased, while diazoxide (DZ) and nitrendipine decreased, $[Ca^{2+}]_i$. In PHHI islets, neither glucose nor tolbutamide caused consistent alterations in $[Ca^{2+}]_i$ whereas in some islets KCl and carbachol increased, and nitrendipine and DZ decreased, $[Ca^{2+}]_i$. Basal $[Ca^{2+}]_i$ in some PHHI islets was elevated with superimposed small amplitude oscillations, unaffected by glucose stimulation. In normal adult islet cells K^+_{ATP} currents were blocked by sulfonylureas and activated by DZ. In contrast, whole cell current recordings and perforated patch recordings of PHHI islet cells revealed only voltage-sensitive currents and no K^+_{ATP} currents, with a membrane potential near 0 mV. Application of DZ caused a 30 mV hyperpolarization but did not activate currents resembling K^+_{ATP}. The DZ-induced alterations in current, membrane potential, and $[Ca^{2+}]_i$ were blocked by glyburide (1 µM). We conclude that the responses to DZ were unrelated to effects on K^+_{ATP} currents. Either human K^+_{ATP} is developmentally regulated or PHHI may be linked to defects in K^+_{ATP} currents.

W-AM-A9

EXPRESSION OF A NEW IRK POTASSIUM CHANNEL IS ESSENTIAL FOR CYTOKINE INDUCED EXPANSION OF HUMAN HEMOPOIETIC PROGENITORS.

(O.Shirihai(1,2),S.Merchav(2),B.Attali(4) and D.Dagan(1,3,5))
Bruce Rappaport Faculty of Medicine, Dept. of Physiol. & Biophysics(1) Unit of Experimental Hemopoiesis(2), Rappaport Institute for Research in the Medical Sciences(3), Weizmann Institute of Science, Dept. of Neurobiology(4) and Bernard Katz Minerva Center for Cell Biophysics(5), Technion, Haifa 31096, Israel. (Spon by E.Braun)

Primitive human hemopoietic progenitor cells expand into lineage-restricted precursors following *in vitro* stimulation by the cytokines Stem Cell Factor and Interleukin-3. A progenitor cell population isolated from human umbilical cord blood was subjected to perforated patch-clamp recordings following overnight incubation with these cytokines. The fraction of cells expressing an inward rectifying potassium channel (K_{ir}) doubled following incubation with both cytokines compared to a background K_{ir} level which was unaltered by incubation with any one of the cytokines alone. Cloning and partial sequencing identified the K_{ir} ion channel as a new member of the IRK family. Antisense oligodeoxynucleotides directed against K_{ir} blocked both mRNA and functional expression of K_{ir} channels. K_{ir} antisense also inhibited the *in vitro* expansion of cytokine-stimulated precursor cells into erythroid and myeloid progenitors in seven day suspension cultures. Extracellular Cs^+ or Ba^{+2}, K_{ir} channel blockers, induced a similar degree of inhibition of progenitor cell generation. These findings strongly suggest an essential role for K_{ir} in the process of cytokine-induced cell growth and differentiation of human hemopoietic progenitors.

W-AM-B1

L-TYPE CALCIUM CHANNELS IN INSULIN-SECRETING CELLS: BIOCHEMICAL CHARACTERIZATION AND PHOSPHORYLATION (*Jörg Striessnig[1], Hannelore Haase[2], Hasan Safayhi[3], Ursel Kramer[3], Andrea Bihlmayer[3], Monika Roenfeldt[3], Hermann P.T. Ammon[3], Ingo Morano[2], Tara N. Cassidy[1] and Michael K. Ahlijanian[4]*)) [1]Institute for Biochemical Pharmacology, University of Innsbruck, Austria;[2]Max-Delbrück Centre for Molecular Medicine, Berlin, Germany; [3]Pharmaceutical Institute, University of Tübingen, Germany; [4]Pfizer Inc., Groton, CT, USA.

Opening of DHP-sensitive voltage-dependent L-type Ca^{2+} channels (LTCCs) represents the final common pathway for insulin-secretion in pancreatic ß-cells. Major biochemical pathways for the modulation of pancreatic LTCCs include phosphorylation (e.g by cAMP dependent protein kinase, PKA) and direct modulation of channel activity by G-proteins. We investigated the subunit structure of (+)-[^{3}H]isradipine labeled LTCCs in insulin-secreting RINm5F cells. Using subunit-specific antibodies we demonstrate that α1C subunits (199 kDa) contribute only a minor portion of the totalα1 immunoreactivity in membranes and partially purified LTCC preparations. However,α1C participates in the formation of the majority of (+)-[^{3}H]isradipine labeled LTCCs as 68% of solubilized (+)-[^{3}H]isradipine binding activity were specifically immunoprecipitated by anti-α1C. Phosphorylation of immunopurified α1C with PKA revealed the existence of a 240 kDa form, that remained undetected in Western-blots and must represent its full length form. Seventy percent of labeled LTCCs were immunoprecipitated by an anti-ß antibody directed against a region conserved in all mammalian ß-subunit isoforms (ß1-ß4). Although ß2 and ß3 immunoreactivity were detected in RINm5F membranes, anti-ß2 (0%) and anti-ß3 antibodies (21%) did not immunoprecipitate substantial portions of binding activity. This subunit composition was similar for DHP-labeled LTCCs in brain but differed from cardiac muscle. In rabbit heart we found 90% of the DHP labeled channels to be associated withα1C and anti-ß2 recognized 42% of the labeled LTCC complexes. We conclude that α1C, and not α1D, is the major constituent of DHP-labeled LTCCs in insulin-secreting cells, its full length form serving as a substrate for phosphorylation by PKA. Our data also demonstrate that different ß-subunits associate with α1C in RINm5F cells and heart muscle. This may account, at least in part, for the differences observed for LTCC function and modulation in these tissues.

(Supported by the Deutsche Diabetes-Gesellschaft (HS), the Fonds zur Förderung der Wissenschaftlichen Forschung (JS), the Graduiertenförderung of Baden-Württemberg (UK), a Fulbright Research fellowship (TNC) and the Deutsche Forschungsgemeinschaft (HH).

W-AM-B2

AN ATP-SENSITIVE Cl^- CURRENT THAT IS ACTIVATED BY CELL SWELLING, cAMP AND GLYBURIDE IN INSULIN-SECRETING CELLS. ((T.A. Kinard and L.S. Satin)) Dept. of Pharm. and Tox., Med. Coll. of VA, Richmond, VA. 23298

Although chloride ions are known to modulate insulin release and islet electrical activity, the mechanism(s) mediating these effects are unclear. However, numerous studies of islet Cl^- fluxes have suggested that Cl^- movements are glucose- and sulfonylurea-sensitive and blocked by stilbene-derivative Cl^- channel blockers. We now show for the first time that insulin-secreting cells have a Cl^- channel current which we term $I_{Cl,islet}$. The current is activated by hypotonic conditions, 1-10 µM glyburide and 0.5 mM 8-bromo-cAMP. $I_{Cl,islet}$ is mediated by Cl^- channels since replacing $[Cl^-]_o$ with less permeant aspartate reduces current amplitude and depolarizes its reversal potential. In addition, 100 µM DIDS, NPPB, niflumic acid or glyburide, which block the Cl^- channels of other cell types, block $I_{Cl,islet}$. Reducing $[ATP]_i$ reduces the amplitude of the current, suggesting that it may be under metabolic control. The current is time-independent and shows strong outward-rectification beyond about 0 mV. At potentials associated with the silent phase of islet electrical activity (≈-65 mV), $I_{Cl,islet}$ mediates a large inward current, which would be expected to depolarize islet membrane potential. Thus, activation of this novel current by increased intracellular cAMP, sulfonylureas or ATP may contribute to the well-known depolarizing effects of these agents. [Supported by NIH DK46409]

W-AM-B3

A ROLE FOR CALCIUM RELEASE-ACTIVATED CURRENT IN PANCREATIC β-CELL BIPHASIC ELECTRICAL ACTIVITY
((D. Mears[1,2], N.F. Sheppard, Jr.[1], E. Rojas[2], I. Atwater[2], R. Bertram[3] and A. Sherman[3])) [1]Department of Biomedical Engineering, Johns Hopkins University, Baltimore, MD 21218, [2]LCBG and [3]MRB, NIDDK, NIH, Bethesda, MD 20892. (Spon. by J. Keizer)

Pancreatic β-cells respond to step increases in glucose concentration with a biphasic pattern of electrical activity consisting of a prolonged depolarization (Phase 1) followed by steady-state oscillations known as bursts. A theoretical study (Bertram et al., Biophys. J. 68:2323) suggests that the transient Phase 1 results from the combined depolarizing influences of potassium channel (K_{ATP}) closure and an inward, non-selective cation current (I_{CRAN}) that activates as calcium stores empty in the absence of glucose. Calcium influx during Phase 1 refills the stores, inactivating I_{CRAN} and allowing steady-state bursting to commence. We support this hypothesis with experimental and theoretical results indicating that Phase 1 duration is sensitive to manipulations that affect the filling of intracellular calcium stores. First, Phase 1 duration increases with duration of glucose deprivation. This phenomenon reflects increased time required to refill calcium stores that have been emptying for longer periods. Second, Phase 1 duration decreases when calcium stores are refilled by exposure to elevated KCl during the glucose removal period. Third, when the rate of store emptying is accelerated by removal of extracellular calcium during the basal glucose exposure, Phase 1 duration increases. Finally, no Phase 1 is observed following exposure to diazoxide in the continued presence of 11 mM glucose, which is consistent with the model since calcium stores remain filled under these conditions (Gylfe, Pflügers Arch. 419:503). Application of muscarinic agonists (which should empty calcium stores and stimulate I_{CRAN}) did not increase Phase 1 duration as the model predicts. Despite this discrepancy, the good agreement between most of the experimental results and the model predictions provides evidence that I_{CRAN} is involved in the transient phase of glucose-induced β-cell electrical activity. (Supported by the Greenwall Foundation)

W-AM-B4

MULTIPHASIC ACTION OF GLUCOSE AND α-KETOISOCAPROIC ACID ON THE CYTOSOLIC pH OF PANCREATIC β-CELLS: EVIDENCE FOR AN ACIDIFICATION PATHWAY LINKED TO THE STIMULATION OF Ca^{2+} INFLUX. ((A.P. Salgado, A.M. Silva, R.M. Santos and L.M. Rosário)) Biochemistry Dept. and Center for Neurosciences, University of Coimbra, P-3049 Coimbra, Portugal. (Spon. by L.M. Rosário)

Glucose stimulation raises the pH_i of pancreatic β-cells, but the underlying mechanisms are not well understood. We have now investigated the acute effects of metabolizable (glucose and the mitochondrial substrate α-ketoisocaproic acid, KIC) and non-metabolizable (high K^+ and the K_{ATP} channel blocker tolbutamide) insulin secretagogues on the pH_i of pancreatic β-cells isolated from normal mice, as assessed by BCECF fluorescence from single cells or islets in the presence of external bicarbonate. The typical acute effect of glucose (22-30 mM) on the pH_i was a fast alkalinization of ca. 0.12 units, followed by a slower acidification. The relative expression of the alkalinizing and acidifying components was variable, with some cells and islets displaying a predominant alkalinization, others a predominant acidification and others yet a mixed combination of the two. The initial alkalinization preceded the $[Ca^{2+}]_i$ rise associated with the activation of voltage-sensitive Ca^{2+} channels, as assessed by combined fura-2 microfluorometry. There was a significant overlap between the glucose-evoked $[Ca^{2+}]_i$ rise and the development of the secondary acidification. Depolarization with 30 mM K^+ and tolbutamide evoked pronounced $[Ca^{2+}]_i$ rises and concomitant cytosolic acidifications. Blocking glucose-induced Ca^{2+} influx (with 0 Ca^{2+}, nifedipine or the K_{ATP} channel agonist diazoxide) suppressed the secondary acidification while having variable effects (potentiation or slight attenuation) on the initial alkalinization. KIC exerted glucose-like effects on the pH_i and $[Ca^{2+}]_i$, but the amplitude of the initial alkalinization was about twice as large for KIC relative to glucose. It is concluded that the acute effect of glucose on the pH_i of pancreatic β-cells is biphasic. While the initial cytosolic alkalinization is an immediate consequence of the activation of H^+-consuming metabolic steps in the mitochondria, the secondary acidification appears to originate from enhanced Ca^{2+} turnover in the cytoplasm. The degree of coupling between glucose metabolism and Ca^{2+} influx as well as the relative efficacies of these processes determines whether the acute pH_i response of a β-cell is predominantly an alkalinization, an acidification or a mixed proportion of the two.

W-AM-B5

MAPPING OF PKA AND CaMKII REGULATORY SITES ON THE GASTRIC ClC-2G Cl^- CHANNEL. ((J. Cuppoletti, E.Y. Kupert, K. Stroffekova, C. Hao, A.M. Sherry, N. Waxham[1] and D.H. Malinowska)). Dept. Mol. & Cell. Physiol. Univ. of Cincinnati Coll. of Med., Cincinnati, OH, USA and [1]University of Texas, Houston, TX, USA.

The voltage- and H^+-activated gastric Cl^- channel (ClC-2G), responsible for Cl^- movement in HCl secretion, has been cloned and expressed (AJP 268 Cell Physiol 37: C191-C200, 1995). The C-terminus of ClC-2G (ca. 500 aa) is rich in potential recognition sequences for PKA and CaMKII. The objectives were to determine whether this region plays a role in channel regulation and which of these sites are responsible for signal transduction through PKA and/or CaMKII. Polypeptides (85-122aa) containing only one phosphorylation site: RRQS or RGCS, presumed PKA and CaMKII substrates; RKS or RIS presumed PKA substrates; and a RGCS->A mutant to serve as a negative control, by recombinant techniques with His tag recognition sequences. The polypeptides were purified, phosphorylated with ^{32}P-ATP using catalytic subunit of PKA or recombinant CaMKII plus Ca^{2+} and calmodulin, and then cleaved with thrombin to remove a potential phosphorylation site within the bacterial fusion protein. Polypeptides with RRQS and RGCS were substrates for both PKA and CaMKII, and RKS and RIS were substrates for PKA. Mutants of the channel with RRQS->H and RKS->L (aa's which differ between ClC-2G and rat brain ClC-2) could not be activated by either PKA or CaMKII. Thus, the C-terminus of ClC-2G is responsible for regulation of ClC-2G, RRQS is responsible for the unique CaMKII activation and RRQS and/or RKS are responsible for PKA activation of the ClC-2G Cl^- channel. Supported by NIH DK-43816, DK-43377 and CF Foundation R457.

W-AM-B6

ANALYSIS OF MAST CELLS SECRETORY RESPONSE TO THE IMMOBILIZATION OF RANDOMLY AND NON-RANDOMLY DISTRIBUTED TYPE I Fc_ε RECEPTORS. ((*Idan Tamir[1], Reinhard Schweitzer-Stenner[2] and Israel Pecht[1]*)) [1] Department of Chemical Immunology. The Weizmann Insitute of Science. Rehovot 76100. Israel; [2] FB1-Institut für Experimentelle Physik. Universität Bremen. 28359 Bremen. Germany. (Spon. by U. Kubitscheck)

Clustering the type I receptor for IgE ($Fc_\varepsilon RI$) on mast cells initiates a cascade of biochemical processes that results in secretion of inflammatory mediators. We have investigated the receptor density and dynamics required from $Fc_\varepsilon RI$ clusters for initiating that cascade. The experimental protocol employed antigen-carrying solid surfaces where the density and mobility of the $Fc_\varepsilon RI$ within the cluster could be controlled. Mast cells (line RBL-2H3) were reacted with these surfaces producing a random distribution of immobilized IgE-Fc_εI complexes on the cells' surface. The cell's secretory response was found to be very sensitive to the density of immobilized $Fc_\varepsilon RI$s, rising rapidly at ca. 1000 immobilized molecules/µm^2. A significant secretory response (25 %) was observed at IgE-densities above 100 molec/µ^2 provided that the corresponding DNP_{11}-BSA surface density exceeds 8000 molec/µ^2. These findings suggest that immobilization of a fraction of the randomly distributed $Fc_\varepsilon RI$s that are in sufficient proximity initiates the stimulatory signal and that this is maintained as long as these receptors are kept within this distance. These results are rationalized in terms of a simple model based on the following assumptions. 1) The cell's surface is divided into square elements of size σ_t. A given constant secretory response is triggered by each cell surface element when occupied by two or more IgE-Fc_εI complexes. 2) The coupling between the active elements and the cells' signalling cascade saturates at high numbers of the active elements. Our analyis shows that two immobilized randomly-distributed $Fc_\varepsilon RI$s constitute a triggering unit for the secretory response provided that their separation distance does not exceed 6 nm.

W-AM-B7

PURINERGIC RECEPTOR EXPRESSION AND FUNCTION IN ADRENAL CHROMAFFIN CELLS: A SINGLE CELL APPROACH. ((L.M. Rosário[1], E. Castro[2], M.T. Miras-Portugal[2], R.M. Barbosa[1], J.A. Stamford[3] and A.R. Tomé[1])) [1]Center for Neurosciences of Coimbra, Portugal; [2]Complutense University of Madrid, Spain; and [3]London Hospital Medical College, UK

We have recently provided evidence that bovine chromaffin cells (CCs) have two types of purinoceptors: a P_{2U}-type receptor, coupled to Ca^{2+} release from internal stores, and a P_2 ionotropic receptor, coupled to fast Ca^{2+} influx (J. Biol. Chem. 270: 5098-5106, 1995). We have now investigated the relative role of these purinoceptors in catecholamine release and the underlying ionic mechanisms. $[Ca^{2+}]_i$ (fura-2) and $[Na^+]_i$ (SBFI) were recorded from single cells by quantitative fluorescence microscopy. Catecholamine release was monitored electrochemically from both cell populations and single cells (the latter *via* carbon fibre microelectrodes). The purinoceptor agonist 2MeSATP evoked $[Ca^{2+}]_i$ rises from a fraction of the ATP-sensitive cells. This effect was strictly dependent upon the presence of external Ca^{2+}, indicating that 2MeSATP activates specifically the P_2 ionotropic receptor in CCs. Both ATP and 2MeSATP evoked catecholamine release in a dose-dependent fashion. The 2MeSATP-induced $[Ca^{2+}]_i$ rises and catecholamine release were suppressed by the P_2 purinoceptor antagonists suramin and PPADS. The specific P_{2U} receptor agonist UTP evoked suramin-insensitive $[Ca^{2+}]_i$ rises from a second fraction of ATP-sensitive CCs but failed to evoke catecholamine release. The ability of ATP to stimulate catecholamine release was restricted to cells possessing the ionotropic purinoceptor, as demonstrated by the simultaneous recording of $[Ca^{2+}]_i$ and secretion from single chromaffin cells. 2MeSATP-evoked catecholamine secretion was abolished by removal of external Ca^{2+} or by replacing Na^+ for NMG^+, suggesting that it is mediated mainly by Na^+ influx, cell depolarization and the activation of voltage-sensitive Ca^{2+} channels. Accordingly, 2MeSATP induced PPADS-blockable rises in $[Ca^{2+}]_i$; furthermore, 2MeSATP-evoked catecholamine release was strongly inhibited by Cd^{2+} at a concentration (0.5 mM) that suppressed high K^+-evoked secretion. It is concluded that ATP-induced catecholamine release from chromaffin cells is exclusively mediated by a cell-specific ionotropic P_2 purinoceptor and that most of this secretion can be accounted for by the activation of voltage-sensitive Ca^{2+} channels.

FOLDING AND SELF-ASSEMBLY: VIRUSES

W-AM-C1

ORGANIZATION OF dsDNA IN BACTERIOPHAGE T7 CAPSIDS: SUPPORT FOR THE COAXIAL-SPOOL MODEL ((M.E. Cerritelli, N. Cheng, A.H. Rosenberg*, M.N. Simon*, and A.C. Steven)) LSB-NIAMS, NIH, Bethesda, MD 20892; *Brookhaven National Lab, Upton, NY 11973. (Spon. by J. Norvell)

In its encapsidated state, the ~40,000 bp genome of bacteriophage T7 is compressed into a sphere of ~550 Å in diameter. We have applied cryo-electron microscopy and scanning transmission EM to investigate its structure. A mutant deleted for genes 11 and 12 produces DNA-filled heads that lack tails. These heads have a tendency to orient on EM grids so that they are viewed along the symmetry axis that passes through the center of the connector. In cryo-micrographs recorded relatively close to focus, these particles present a distinctive pattern of concentric circles or spirals with the characteristic 26 Å spacing that corresponds to lateral packing of DNA duplexes [1]. 77 such images were analyzed by correlation averaging. Icosahedral orientation analysis confirmed that they were indeed viewed along or close to a 5-fold axis. The resulting feature enhancement in the averaged image indicates that the DNA is packaged in a rather consistent manner from particle to particle. This projection is in agreement with a spool model for packaged DNA [2,3], where the winding of the DNA is coaxial with the connector and internal protein core. In support of this interpretation, treatment with cobalt-tungsten stain disrupts the heads, resulting in the release of packaged DNA in a compact, highly-ordered state, as seen in the STEM. In axial views of disrupted heads, sets of parallel curved striations arising from aligned DNA duplexes are clearly evident. It remains to be determined whether the regularities we observe in the packaged DNA structure are unique to T7 and are dependent on the presence of an internal protein core.

1. Booy, F. P., Trus, B. L. et al (1992) EMSA pp. 452-453.
2. Richards, K. E., Williams et al (1973) J. Mol. Biol. 78, 255-259.
3. Earnshaw, W. C. and Harrison, S. C. (1977) Nature 268, 598-602.

W-AM-C2

THE CONFORMATION OF PACKAGED BACTERIOPHAGE G DNA. ((M. Sun and P. Serwer)) The Univ. of Texas Hlth. Sci. Ctr. at San Antonio, Texas 78284-7760. (Spon. by B. Goins)

The double-stranded DNA packaged in the capsids of some bacteriophages is contained in a space that has a volume roughly twice the volume of the packaged DNA double helix. To reduce the resolution needed to observe DNA domains within packaged DNA, we have observed DNA packaged in a comparatively large bacteriophage, called G (length of DNA = 670 kb). In negatively stained specimens of bacteriophage G, electron microscopy reveals packaged DNA discontinuities that are explained by the presence of folds in the DNA double helix. In positively stained specimens, some particles have DNA-associated stain in relatively high concentration near the corners of the polyhedral bacteriophage G capsid. This observation supports the assumption of folded DNA regions. When ultraviolet light-induced DNA-DNA cross-linking is performed before expulsion of DNA, some partially unraveled DNAs are found to have one of the following two types of appearance: (a) a central zone of compacted DNA that is surrounded by multiple loops of DNA, and (b) a branched filament that consists of parallel bundles of double helical DNA segments. The bundles do not exhibit any winding around each other. Both the loops and the branched filament appear to require folding (in contrast to winding) of the DNA packaged in a bacteriophage G capsid. The central, compact zone of some partially unraveled G DNAs requires the folding to have inside-to-outside polarity. Supported by NSF-MCB 9316660.

W-AM-C3

FORMATION OF A PCR-SPECIFIED HYBRID BACTERIOPHAGE BY IN VITRO RECOMBINATION-PACKAGING. ((S. A. Khan, R. H. Watson, S. J. Hayes, and Philip Serwer)) The Univ. of Texas Hlth. Sci. Ctr., San Antonio, Texas 78284-7760.

The tail fiber of bacteriophage T7, but not the tail fiber of the T7-related bacteriophage, T3, adheres the bacteriophage to agarose gels during agarose gel electrophoresis. To avoid this adherence, we have developed a procedure of in vitro recombination-packaging by which part of the gene for the T3 tail fiber was transferred to the T7 genome. After using the polymerase chain reaction (PCR) to amplify the tail fiber-encoding T3 gene 17, the T3 PCR fragment was incubated in a DNA packaging extract (1), together with purified T7 DNA that had an amber mutation in gene 17. Bacteriophage produced after both in vitro recombination and in vitro packaging were plated on a host nonpermissive for amber mutants. By oligonucleotide hybridization to plaques, T7-T3 hybrid bacteriophage were identified. These bacteriophage had lost the T7 agarose gel-adherence phenotype. By nucleotide sequencing, the T3 DNA fragment transferred was found truncated at both ends. Thus, the recombination-packaging process appears to sample different regions of the PCR fragment for transfer with viability; for example, transfer of the whole gene 17 might be lethal. This latter feature is advantageous for construction of viral hybrids, in general. By use of a PCR fragment produced under mutagenic conditions, in vitro recombination-packaging has also been used for region-specific mutagenesis. Supported by NSF-MCB 9316660.

1. M. Son, R. H. Watson, and P. Serwer (1993) Virology 196, 282-289.

W-AM-C4

STRUCTURAL ORGANIZATION OF PROTEIN AND DNA IN FILAMENTOUS BACTERIOPHAGE M13
((G.P.Kishchenko and L. Makowski)) IMB, FSU, Tallahassee, FL 32306-3015

Fiber diffraction patterns from magnetically oriented fibers of M13 particles were analyzed. All diffraction data occured on layer lines with a 33.1 Å repeat indicating that both the major coat protein and the DNA have this axial periodicity. Intensities along layer lines were obtained by angular deconvolution. A model of the virion has been constructed and refined to beyond 4.5 Å resolution. The major coat protein is largely α-helical with symmetry C_5S_2 and a 33.1 Å pitch. The C-terminal portions of the coat proteins form the inner surface of the virus where they interact in a head-to-tail manner to form almost continuous five-stranded helices. This organization of the viral interior suggests a simple model for DNA organization within the phage particale in which the single-stranded viral DNA is inscribed within the protein coat with 12 bases per turn and a 33.1 Å pitch. The DNA phosphates are 11 Å from the viral axis. The duality of protein and DNA structures form a particle with an approximate 33.1 Å axial repeat. In this particle, adjacent phosphates are not strictly equivalent because they interact with different parts of the coat proteins. Rather, they are related to the C-terminal protein helices in approximately the same way, providing a flexibility of interaction that expresses itself in particles with varying protein to DNA ratios.

W-AM-C5

DETERMINATION OF SUBUNIT AND SIDE CHAIN ORIENTATIONS IN *Ff* FILAMENTOUS VIRUS BY POLARIZED RAMAN MICRO-SPECTROSCOPY OF ORIENTED FIBERS. ((S. A. Overman, M. Tsuboi and G. J. Thomas, Jr.)) Division of Cell Biology and Biophysics, School of Biological Sciences, University of Missouri, Kansas City, MO 64110.

The *Ff* filamentous viruses (*fd, M13, f1*) are important models for membrane protein assembly and are used extensively as cloning vectors and vehicles for peptide display. The threadlike virion (≈6 x 880 nm) comprises a single-stranded DNA genome sheathed by ≈2700 copies of a 50-residue α-helical subunit (pVIII). The inclination of pVIII from the virion axis and the orientation of its unique tryptophan side chain (W26) within the assembled virion have been determined experimentally from polarized Raman spectra of oriented *fd* fibers obtained on a Raman microscope. The Raman polarizations have been interpreted by use of local Raman tensors for peptide group vibrations (amide I and amide III) and tryptophan ring vibrations (normal modes *W3*, *W7* and *W7'*). We find that the average tilt of the pVIII α-helix from the virion axis is ≈15°, consistent with previous estimates based upon solid state NMR and X-ray fiber diffraction data. We also find that the indole ring of the W26 side chain is close to parallel to the virion axis with the N1-C2 endocyclic bond approximately perpendicular to the axis. In combination with the previously determined value for the tryptophan C2-C3-Cβ-Cα dihedral angle (torsion $\chi^{2,1}$), a detailed molecular model is proposed for the conformation and local environment of residue W26 in the native *Ff* assembly. [Supported by NIH Grant GM50776.]

W-AM-C6

KINETIC MODELING OF VIRUS CAPSID ASSEMBLY.((B. Berger[1], R. Schwartz[1] , P.W. Shor[2] ., P.E. Prevelige Jr.[3])) [1]MIT, Cambridge, MA ; [2]AT&T Bell Labs, Murray Hill, NJ;.[3]Univ. of Alabama, Birmingham AL

The assembly of icosahedral viral capsid from subunits is complex in comparison to the assembly of helical polymers such as actin, tubulin, and helical viruses due to the need for subunit conformational switching to be coupled to subunit addition. The subunits of an icosahedral capsid of T >1 are in different symmetry environments; we propose that during assembly, the subunits assume distinct conformations in response to binding interactions with their immediate neighbors. This in turn determines the binding environments for successively added subunits, eventually guaranteeing successful assembly

A computer program implementing a model based on a "local rules" system of assembly has been developed (Berger et al., PNAS, 91, 1994, 7732--7736). In this model all information necessary to determine the conformation of a subunit being added is provided by subunits in direct contact with it, and/or the presence of specified scaffolding subunits. Computer experiments using this model have demonstrated that various slight pertubations in the binding interactions of a single subunit are each sufficient to interfere with successful assembly. We are extending the modelling program to include kinetic factors in order to produce experimentally testable predictions which will distinguish between different models of the assembly pathway. Some questions we will address are: Do the kinetics differ if subunits add at a single growing point or at multiple growing points. The effect on the overall kinetics and the probability of assembly if the relative binding constants of the subunits depend on their target conformation. What is the minimal relative binding constant for a "poison subunit" necessary to successful inhibit assembly.

W-AM-C7

REGULATION OF HEPATITIS B VIRUS CORE ASSEMBLY AND POLYMORPHISM. ((A. Zlotnick, N. Cheng, J.F. Conway, F.P. Booy, A.C. Steven, S.J. Stahl[2], and P.T. Wingfield[2])) Laboratory of Structural Biology, NIAMS, NIH, Bethesda, MD 20892, [2]Protein Expression Laboratory, NIH, Bethesda, MD 20892 (Spon. J. E. Johnson)

The capsid of Hepatitis B Virus (HBV) is a homopolymer of core protein dimers. *In vivo* and *in vitro*, core protein can self-assemble into icosahedra of two different sizes, T=3 (90 dimers) and T=4 (120 dimers)*. Cryo-EM image reconstructions of T=3 and T=4 particles were calculated to 18 Å resolution. Half-dimers are arranged in groups of five or six with fivefold and quasi-sixfold symmetry, respectively. Dimers, considered individually, and the arrangement of fivefold axes were essentially identical. Quasi-sixfold groupings were distinct between T=3 and T=4 particles and may be described as having chair and boat conformations, respectively. The physical chemical basis of assembly and polymorphism was investigated using three different genetic constructs of core protein, C-terminally truncated to different extents. Dissociated dimers were polymerized by lowering pH to near neutral and increasing the ionic strength. Each construct had a characteristic T=3/T=4 ratio ranging from ~10/90 to ~70/30, with T=4 particles favored by longer C-termini. T=3 and T=4 particles were stable; purified particles did not re-equilibrate. The ratio was also insensitive to the initial dimer concentration. Thus, assembly was under kinetic control, and the C-terminus was shown to be an important structural determinant for the T=3/T=4 ratio.

* Crowther et al (1994), Cell 73, 943. Wingfield et al (1995), Biochemistry 34, 4919.

W-AM-C8

THREE-DIMENSIONAL STRUCTURE OF SCAFFOLDING-CONTAINING PHAGE P22 PROCAPSIDS BY ELECTRON CRYO-MICROSCOPY ((P. A. Thuman-Commike[1], B. Greene[2], J. Jokana[1], B. V. V. Prasad[1], W. Chiu[1];, J. King[2], P.E. Prevelige Jr.[3]))[1] Baylor College of Medicine, Houston TX; [2]MIT, Cambridge MA.; [3]Univ. of Alabama Birmingham, Birmingham AL (Spon by J. Lebowitz)

Electron cryo-microscopy has been used to study the three-dimensional structures of the bacteriophage P22 procapsids containing wild-type and mutant scaffolding proteins. The scaffolding mutant structure has been resolved to 19 Å resolution and agrees with the 22 Å resolution wild-type procapsid reconstruction. Both procapsid reconstructions contain an outer icosahedral coat protein shell and an inner scaffolding protein core. The outer coat protein forms a T = 7 icosahedral lattice of pentons and skewed hexons. Computational isolation of the skewed hexon shows the presence of a local two-fold axis which reduces the number of unique subunits in the asymmetric unit to four at this resolution. The four unique subunits, all composed of one protein, have been classified into three distinct classes based upon the upper domain's shape, and the presence of a channel leading to the inner surface. At the inner surface of the coat protein finger-like regions which extend towards the scaffolding protein core may indicate an interaction point with the internal scaffolding subunits. Analysis of the internal scaffolding protein core in these reconstructions does not show any evidence of strong icosahedral dispostion. However, it is possible that there is a pseudo icosahedral interaction between the coat and scaffolding proteins near the inner surface of the coat shell.

W-AM-C9

ELECTRON CRYSTALLOGRAPHY OF THE ROTAVIRUS INNER CAPSID PROTEIN VP6 *((George G. Hsu[t], A. Richard Bellamy[#] and Mark Yeager[t]))*
[t]The Scripps Research Institute, Dept. of Cell Biology, La Jolla, CA 92037.
[#]School of Biological Sciences, Univ. of Auckland, Auckland, New Zealand.
(Spon. by M. Tihova)

Rotavirus is one of the most significant causes of death in young children and infants as a result of severe gastroenteritis. The structural proteins in rotavirus are organized into three layers: outer and inner capsid shells, and a virus core which encapsidates the dsRNA segmented genome. In the cytoplasm of infected cells, immature inner capsid particles (ICPs) assemble with a surface formed by 260 trimers of VP6, a 45 kDa protein arranged on a T=13*l* icosahedral lattice. Assembly of mature virions occurs in the lumen of the endoplasmic reticulum (ER). Targeting of the ICP to the ER is mediated by a virally encoded glycoprotein receptor (NSP4). A detailed structure of VP6 will be essential for understanding the interactions between VP6 and NSP4. To this end, we are using electron crystallography to examine two-dimensional crystals (2-D) of VP6. Rotavirus strain SA11 ICPs were treated with 1.5M $CaCl_2$ in 10mM Tris-HCl buffer at pH 8.0, and the released VP6 was purified by CsCl gradient ultracentrifugation. 2-D crystals were grown by sequential dialysis against (1) 10mM NaPi buffer at pH 6.0 containing 0.2M EDTA and 0.02% NaN_3 and then (2) 10mM Tris-HCl pH7.4 containing 0.02% NaN_3. Electron micrographs of negatively stained 2-D crystals were recorded using minimal dose techniques. Optical diffraction was used to select the most crystalline areas, which were digitized and corrected for lattice distortions. The refined unit cell parameters were a=101±1.0Å, b=103±1.9Å and γ=118±1.5°. To a resolution of 15Å, the phase error for p2 plane group symmetry was 11.2°. Projection density maps show that VP6 is trimeric, as is seen in the icosahedral ICPs. The trimers have an edge length of ~70Å, and the roughly circular subunits have a diameter of ~35Å. Determination of the 3-D structure is being performed by the method of tilt reconstruction. Glucose-embedded crystals display diffraction to ~6Å resolution so that a higher resolution analysis should be feasible.

W-AM-D1

CHAOS IN THE CRAYFISH SIXTH GANGLION†

((Xing Pei and Frank Moss)) Laboratory for Neurodynamics, University of Missouri at St. Louis, St. Louis, MO 63121

Chaos in biological systems has received attention since the early 1980s. While most studies have been criticized, the topic remains of interest, especially to medical scientists, since successful techniques for characterizing chaos might lead to new therapies or diagnostics. Recently a new technique, quite different in substance from conventional methods most of which measure Lyapunov exponents or fractal dimensions, has been put forth[1,2]. Evidence for chaos is obtained by observing periodic orbits near unstable fixed points. Such points are buried in a sea of random noise, so that convincing detection becomes a statistical problem[3]. The method easily distinguishes noise contaminated chaos from noisy limit cycles[3]. Here we apply the technique to the detection of chaos in the 6th ganglion of the crayfish *Procambarus clarkii*. This abdominal ganglion consists of a few hundred interneurons and a pair of bilaterally symmetric photoreceptors. The interneurons receive presynaptic input from hydrodynamically sensitive hair mechanoreceptors, which we periodically stimulate, while recording postsynaptically from the photoreceptor output. Regions of chaotic behavior are mapped out in the parameter space of stimulus amplitude and frequency and light intensity falling on the photoreceptor.

†Supported by the Office of Naval Research Program in Nonlinear Physics

1. S. J. Schiff, *et al*, *Nature*, 370, 615-620 (1994)
2. F. Moss, *Nature*, 370, 596-597 (1994)
3. D. Pierson and F. Moss. *Phys. Rev. Lett.*, 75, 2124-2127 (1995)

W-AM-D2

EVOKED HAIR-BUNDLE MOTILITY DURING MECHANOELECTRICAL TRANSDUCTION IN HAIR CELLS OF THE BULLFROG'S SACCULUS.

((Robert Marquis, Michael E. Benser, and A. J. Hudspeth)) Howard Hughes Medical Institute and Laboratory of Sensory Neuroscience, The Rockefeller University, New York, NY 10021-6399.

The hair bundle is the organelle responsible for mechanoelectrical transduction in the hair cell, the receptor of the vertebrate acousticolateralis system. Displacement of a hair bundle toward its tall edge opens transduction channels, allowing cations to flow into and depolarize the cell. When pulled in this direction by a flexible fiber, the bundle initially follows the stimulus, but then transiently changes direction and jerks the fiber backwards. In order to investigate the relationship between this "twitch" and mechanoelectrical transduction, we made simultaneous recordings of hair-bundle motion and the receptor potential. Only the healthiest cells, as judged by their morphology, resting membrane potential, and sensitivity to small stimuli, exhibited twitches. A twitch was always associated with a depolarizing receptor-potential spike of similar time course. Both phenomena were labile, exhibited saturation with large stimuli, and depended upon the bundle's resting position and rate of deflection. As an index of the transduction current, we measured the initial slope of the receptor potential prior to the activation of voltage-sensitive ion channels. The twitch's magnitude was greatest over the range of bundle displacements in which the transduction current grew most rapidly. These results suggest that transduction is most sensitive when the hair bundle responds actively to a stimulus. Hair-bundle motility may not only increase the sensitivity of a stimulated hair cell, but also generate force in the mechanical feedback system, or cochlear amplifier, responsible for our finely tuned sense of hearing.

This research was supported by NIH grant DC00241.

W-AM-D3

GATING KINETICS OF A HAIR CELL'S MECHANOSENSITIVE CHANNELS AND ACTIVE HAIR-BUNDLE MOTION.

((Vladislav S. Markin and Michael E. Benser)) Departments of Anesthesiology and Pain Management and Biomedical Engineering, University of Texas Southwestern Medical Center, Dallas, Texas 75235-9068.

The standard description of the hair cell's mechanoelectrical-transduction channel's open probability is given by a Boltzmann function depending on hair-bundle displacement. Because, upon a bundle's protracted displacement, the channel's open probability adapts to its resting level with a time constant of ~20 ms, the applicability of this function is restricted to short times. Based on the hair bundle's unique "twitch" response to its abrupt deflection (Marquis *et al.*, *Biophys. Soc.*, 1996) and a concomitant sharp increase in transduction-channel opening (Howard and Hudspeth, *Proc. Natl. Acad. Sci. USA*, 84: 3064, 1987), we conclude that the standard function is not applicable during the initial few milliseconds of a bundle's displacement, as well. To describe the variation of the channel's open probability in the first few milliseconds of a bundle's displacement, we augmented the standard function with an activation parameter, c, that has first-order kinetics:

$$p_0(X,c) = 1/\left\{1+\exp\left[(X_0 - X)/\Lambda - d\exp(aX - bc)\right]\right\}$$

When supplemented with a dynamic equation of hair-bundle stimulation including adaptation, our model was able to simulate, in good quantitative agreement, the change in transduction-channel open probability and the bundle's twitched motion over both short and long time periods. Our model suggests the bundle's active twitching motion may be manifested solely from the forces within the channel's elastic gating elements. Active hair-bundle motion may, in turn, underlie cochlear amplification.

This research was supported by National Institutes of Health grant DC00317.

W-AM-D4

MECHANOSENSITIVE CATIONIC CHANNELS FROM ENDOTHELIUM OF EXCISED INTACT RAT AORTA.

((S.M. Marchenko and S.O. Sage)) Physiological Laboratory, University of Cambridge, Cambridge, CB2 3EG, UK. (Spon. by C.W. Taylor)

Single channels were recorded in endothelium of excised intact rat aorta using the patch clamp technique. One major type of cationic channel was present in cell-attached patches of unstimulated endothelium. Negative pressure applied to the patches through the pipette inhibited activity of the channels whereas positive pressure increased their open probability. Therefore the channels response to pressure depended on the stimulus direction. This suggests involvement of a gating mechanism that does not depend on stretch of the membrane, but may include interaction of the channel with cytoskeletal elements normal to the membrane. In this respect they differ from stretch-activated channels previously described in endothelial cells as well as from all other reported stretch-activated and stretch-inactivated channels. Their activity in unstimulated patches were 36.8 ± 12.4 % (mean ± s.e., n=23) of the maximum achieved with positive pressure. The same channels were present in excised inside-out patches, but we could not record them in outside-out patches, probably due to large damage of cytoskeleton in these patches. The current-voltage relationships of the channel demonstrated inward rectification with a slope conductance for inward current of 33.8 ± 3.9 pS (mean ± s.e., n=11). The reversal potential in inside-out patches was close to 0 mV when intrapipette and extrapipette solutions contained (mM) 150 NaCl, 3 KCl, 10 HEPES, 1 EGTA and 150 KCl, 3 NaCl, 10 HEPES, 1 EGTA respectively, pH 7.35. This suggests equal permeability of the channel to Na^+ and K^+. Inward single channel currents, inactivated by negative and activated by positive pressure could be recorded when patch pipettes were filled with isotonic $CaCa_2$ solution, indicating permeability of the channels to Ca^{2+}. The Ca^{2+} permeability of these channels may provide a second messenger mechanism by which they may affect endothelial function. (Supported by The Wellcome Trust).

W-AM-D5

PULSATILE FLUID FLOW-INDUCED SHEAR STRESS INCREASES INTRACELLULAR CALCIUM CONCENTRATION IN BOVINE ARTICULAR CHONDROCYTES

((C.E. Yellowley, C.R. Jacobs, Z. Zhou and H.J. Donahue)) Musculoskeletal Research Laboratory, Department of Orthopaedics and Rehabilitation, Penn State College of Medicine, Hershey, PA 17033. (Spon. by J.C.Hancox)

It has been suggested that mechanical signals, which regulate chondrocyte metabolism, are transduced via fluid flow-induced shear stress. However, the signal transduction mechanisms involved are unknown. To address this issue we investigated the effects of pulsatile fluid flow on intracellular calcium ion concentration ($[Ca^{2+}]_i$) in bovine articular chondrocytes. Cells were loaded with Fura-2 AM and exposed to pulsatile (0.5Hz) fluid flow which induced shear stresses of 0, 10, 20 or 37 dynes/cm^2. Fluorescent intensities at 340 and 380nm, the ratio of which reflects $[Ca^{2+}]_i$, were recorded for individual cells. At zero flow (control) only 2% of cells showed a response (greater than 25% increase in Fura 340/380 ratio over basal), whereas 6% of cells responded to 10 dynes/cm^2, 17% responded to 20 dynes/cm^2 and 32% responded to 37 dynes/cm^2 ($p<0.001$ versus control). The mean $[Ca^{2+}]_i$ increase in responding cells was similar at all shear stresses. These data suggest that fluid flow-induced mobilization of Ca^{2+}_i may contribute to the mechanism by which mechanical loads are transduced to chondrocytes.

W-AM-D6

CURVATURE-SENSITIVE MECHANOSENSITIVE ION CHANNELS AND OSMOTICALLY-EVOKED MOVEMENTS OF THE PATCH MEMBRANE

((C.L. Bowman[1] and J.W. Lohr[2])) 1. Department of Biophysical Sciences, SUNY-Buffalo, 2. VAMC, Buffalo, New York 14214.

Curvature-sensitive (CS) mechanosensitive ion channels appear to sense membrane tension only when the patch membrane is curved toward the soma (Bowman et al. Brain Res. 584: 272-286, 1992). When the membrane is in this permissive configuration, increases in pipette pressure evoke increases in channel activity. In the present study, cell-attached patches (gigaseals) were formed using C6 glioma cells. The patch membrane was examined at ~ 2500x using DIC microscopy. Images of the patch, ion channel activity, and pressure were recorded simultaneously. Channel activity increased with increases in pressure when the patch membrane was curved toward the soma. By contrast, no channel activity was observed when the patch was curved away from the soma. Multiple conductances were observed. Each conductance reversed at a membrane potential of ~ 0 mV. Outward currents were easily observed. CS channels were easily distinguishable from the 40 pS stretch-activated channels (SA) present on these cells since the conductances of CS channels were substantially larger, and the reversal potentials were more negative. SA and CS channels sometimes appear in the same patch. Osmotic stimulation (hypotonic bath solution) causes the cells to swell with concomitant movement of the patch membrane toward the tip of the electrode. During this movement, the gigaseal is always maintained and the direction of curvature of the patch membrane can reverse to the permissive direction. After such reversal, multiple conductance channel activity is observed provided the osmotic stimulus is large enough (~ 150 mOsmol change). The osmotically-evoked movement of the patch membrane demonstrates mechanical coupling between the cell and patch. The movement of the patch membrane is against the flow of water from the cell into the isotonic pipette solution. The force exerted on the patch membrane/cytoskeleton by the cell swelling dominates the force exerted on the patch membrane by the flux of water into the pipette.

W-AM-D7

Mutations that change gating properties of a mechanosensitive channel in *E. coli* ((Paul Blount[1], Sergei Sukharev[1], Matthew Schroeder[1], Scott Nagle[2], and Ching Kung[1,3])) Laboratory of Molecular Biology[1], and Dept. of Genetics [3], Univ. of Wisconsin, Madison, WI 53706, USA. SN's current address is the University of Chicago School of Medicine[2]

Two mechanosensitive channel activities have been found in the envelope of *E. coli* by patch-clamping giant spheroplasts. One of the activities is called MscL for a MechanoSensitive Channel of Large conductance; the other, with smaller conductance, is called MscS. Previously, we cloned and sequenced the gene whose expression has been shown to be necessary and sufficient for MscL activity (*Nature*, 1994, **368**, 265). This gene (*mscL*) encodes a protein of 136 amino acids with two large hydrophobic domains encompassing the first two-thirds of the molecule. Because the MscL protein forms a large pore (~2.2nS) through which ions may pass, hydrophilic domains may be important for function. We have begun to investigate some of the hydrophilic domains of this protein by deletion and point mutations. Three different regions were targeted: a single charged amino acid in the middle of a putative transmembrane domain, a hydrophilic residue in a putative pore region, and the hydrophilic carboxyl tail domain. Analysis of deletion mutants demonstrated that much of the hydrophilic carboxyl domain appears **not** to contribute to MscL activity. In contrast, when the single amino acid mutations were analyzed, MscL activities were observed with significantly longer or shorter open times, or increased or decreased mechanosensitivity, suggesting that these regions are involved in channel gating. (Supported by NIH grant GM47856; PB is a DOE-energy biosciences research fellow of the Life Sciences Research Foundation.).

W-AM-D8

MULTIMERIC STRUCTURE OF BACTERIAL MECHANOSENSITIVE CHANNEL MscL. ((Sergei I. Sukharev,* Paul Blount,* Matthew Schroeder* and Ching Kung*†)) *Laboratory of Molecular Biology and †Department of Genetics, University of Wisconsin, Madison, WI 53706.

Subunit composition and structural symmetry or asymmetry are important features for function of many channels. For MscL, a large-conductance mechanosensitive channel of *E. coli*, we have shown that the expression of only one molecular component, a relatively short (15 kD) protein, is necessary (*Nature*, 1994, **368**:265). The protein has two predicted transmembrane domains with a putative amphiphilic P domain between them. The large conductance of this channel (~2.5 nS in 400 mM KCl) implies multimerization. After preliminary assessment of the size of the functional MscL complex by size-exclusion chromatography in non-denaturing conditions as 50-100 kD, we pursued covalent crosslinking and genetic approaches. Crosslinking of affinity-purified 6His-MscL complexes with DSS revealed 5 additional incrementally spaced bands in SDS gels. The same pattern was obtained after crosslinking of unmodified MscL complexes *in situ* (in native membranes) with subsequent visualization by Western blot technique. Tandem duplication and triplication of *mscL* coding region within one ORF resulted in expression of functional channels consistent with the hypothesis that the number of subunits in the complex is multiple of 2 and 3. These data strongly suggest a hexameric stoichiometry of channel assembly. (Supported by NIH GM47856; PB is a DOE-energy biosciences fellow of the Life Sciences Research Foundation)

MEMBRANE TRANSPORT

W-AM-E1

ΔpH AND ABSOLUTE pH STRONGLY INFLUENCE Ca^{2+} TRANSPORT CATALYZED BY IONOPHORES : A23187, 4-BrA23187, AND IONOMYCIN DO NOT READILY EQUILIBRATE ΔpCa AND ΔpH (D.R. Pfeiffer and R.W. Taylor) Department of Medical Biochemistry, The Ohio State University, Columbus, OH 43210, and Department of Chemistry and Biochemistry, University of Oklahoma, Norman, OK 73019.

Phospholipid vesicles loaded with Quin-2 and BCECF have been utilized to investigate the effects of pH conditions on the Ca^{2+} transport properties of A23187, 4-BrA23187 and ionomycin. At an external pH of 7.0, a ΔpH (inside basic) of ~0.5 U decreases the initial rate and the extent of Ca^{2+} transport into the vesicles. In contrast, raising the pH by 0.5 U in the absence of a ΔpH increases both parameters. The effects of ΔpH on the transport properties of Ca^{2+} ionophores appear to reflect a partial equilibration of the transmembrane ionophore distribution with the H^+ concentration gradient across the vesicle membrane. This unequal distribution of ionophore, together with a second factor, limits the equilibration of ΔpCa and ΔpH produced by the Ca^{2+} ionophores. The extents of nonequilibration are large at physiological pH and grow larger as the pH is increased. They are also inversely related to the ionophore concentration. These findings suggest that Ca^{2+} ionophores should not be used to calibrate intracellular fluorescent probes and that the "null point titration" technique will give erroneous values for the intracellular concentration of divalent cations. (Supported by USPHS Grant HL49182)

W-AM-E2

4-BrA23187, BUT NOT A23187 OR IONOMYCIN, IS HIGHLY SELECTIVE FOR THE TRANSPORT OF TRANSITION METAL CATIONS (W.L. Erdahl, C.J. Chapman, R.W. Taylor and D.R. Pfeiffer) Department of Medical Biochemistry, The Ohio State University, Columbus, OH 43210, and the Department of Chemistry and Biochemistry, University of Oklahoma, Norman, OK 73019..

Transition metal cations play important roles in metabolism, influence gene expression, and may participate in cell signaling. Methods to specifically manipulate these cations in cells are needed to further investigate their biological roles. 4-BrA23187 transports transition metal cations into phospholipid vesicles with the selectivity sequence $Zn^{2+} > Mn^{2+} > Cu^{2+} > Co^{2+} >> Ca^{2+} \approx Ni^{2+}$. The transport selectivity for Zn^{2+} and Mn^{2+} over Ca^{2+} is pH dependent, reaching a maximum near pH 6.7. It is also dependent on the cation concentration, reaching a maxium near 100 μM. Although not yet optimized for ionophore concentration, transport selectivity ratios (Zn^{2+}/Ca^{+} or Mn^{2+}/Ca^{2+}) approaching 2×10^3 have already been observed. Under comparable conditions, the ratios for A23187 and ionomycin are only ~20-50. 4-BrA23187 displays a pK_a of ~6, compared to a value of 7.85 for A23187. A 1:1 complex between 4-BrA23187 (but not A23187) and Zn^{2+} or Mn^{2+} appears responsible for a fraction of the transport. These factors partially explain the high transport selectivity for Zn^{2+} and Mn^{2+}. 4-BrA23187 may be useful for pertubing intracellular levels of Zn^{2+} and Mn^{2+} without altering the intracellular concentration of free Ca^{2+}. (Supported by USPHS Grant HL49181)

W-AM-E3

THE TRANSPORT OF LANTHANIDE CATIONS BY THE Ca^{2+} IONOPHORES A23187, 4-BrA23187 AND IONOMYCIN (Exing Wang and Douglas R. Pfeiffer) Department of Medical Biochemistry, The Ohio State University, Columbus, OH 43210.

Phospholipid vesicle model transport systems allow the mechanism and selectivity of cation transport by ionophores to be determined under conditions similar to those encountered in biological systems. Quin-2 loaded vesicles prepared from 1-palmitoyl-2-oleoyl-*sn*-glycero-phosphatidylcholine, by extrusion techniques, have been used to show that ionophores A23187, 4-BrA23187 and ionomycin transport trivalent lanthanide cations with about 10% of the activity displayed for Ca^{2+}. This activity range is subject to variation depending upon the cation in question and the prevailing conditions. The rate of lanthanide cation transport shows an unusual inverse dependence on the cation concentration. In addition, plots of log rate vs. log ionophore concentration are nonlinear, with slopes ranging from ~1 to ~3 within different segments of the curves. The observed value of H^+ to M^{3+} transported is 2.0. Furthermore, agents and conditions which collapse $\Delta\psi$ accelerate transport. These data indicate that lanthanide cations are transported through a mixture of electrogenic and electroneutral modes. Caution is warranted when using lanthanide cations and Ca^{2+} ionophores simultaneously to investigate cell regulation by Ca^{2+} (Supported by USPHS Grant HL49181)

W-AM-E4

aqpZ WATER CHANNEL PROTEIN FROM *E. coli*. ((G. Calamita, W.R. Bishai, G.M. Preston, W.B. Guggino, and P. Agre)) Johns Hopkins School of Medicine and School of Hygiene and Public Health, Baltimore, MD 21205 (Spon. by S.M. Green)

Evolutionary studies suggest a common prokaryotic origin for the aquaporin family of water channels. Although the *E. coli* glycerol facilitator (glpF) is sequence-related, it does not exhibit selective water transport. We isolated a DNA fragment from *E. coli* with a 693 bp sequence encoding a protein 26-37 % identical to known aquaporins. Like known aquaporins, the deduced aqpZ polypeptide has six transmembrane domains and five connecting loops, but no cysteines at known mercury-sensitive sites. When compared to plant and mammalian aquaporins, aqpZ contains an additional nine residue cassette preceding exofacial loop C and truncated NH_2- and COOH-termini. Expression of aqpZ in *Xenopus* oocytes caused a 15-fold increase in osmotic water permeability (P_f) which was not inhibited by $HgCl_2$ and exhibited a low activation energy (E_a = 3.8 kcal/mol). No uptake of urea or glycerol was detected in oocytes expressing aqpZ, whereas significant glycerol uptake was observed with oocytes expressing glpF. Genomic Southern analysis of bacteria probed with aqpZ revealed putative aqpZ homologs in gram-positive and -negative species. Thus, bacteria apparently express two sequence-related genes with distinct transport functions, a glycerol facilitator gene (glpF) and an aquaporin gene (aqpZ); phylogenetic comparisons indicate that glpF and aqpZ are descendants of an early evolutionary divergence. Future studies of aqpZ expression may elucidate specific roles of aquaporins in bacteria, and comparative analyses of glpF and aqpZ structures may provide insight into how these proteins function.

W-AM-E5

LATERAL MOBILITY OF AQUAPORIN-1 WATER CHANNEL PROTEIN IN MEMBRANES OF INTACT HUMAN RED BLOOD CELLS. ((M.R. Cho, B.L. Smith, J.J. Moulds, P. Agre and D.E. Golan)) Depts. of Biol. Chem. & Mol. Pharm. & of Medicine, Harvard Medical School, Div. of Hematol.-Oncol., Brigham & Women's Hospital, Boston, MA 02115; Depts. of Medicine & of Biol. Chem., Johns Hopkins University School of Medicine, Baltimore, MD 21205; Gamma Biologicals Inc., Houston, TX 77092

AQP1 is the first characterized member of the aquaporin family of membrane water channels. We used the fluorescence photobleaching recovery technique to investigate the lateral mobility of AQP1 in membranes of intact human red blood cells (RBCs). Anti-AQP1 IgG (anti-Co3) was affinity purified from the plasma of a Colton negative, type O individual, and conjugated to FITC. FITC-anti-AQP1 was used to label AQP1 in intact human RBCs. Colton negative RBCs showed defective water channel expression and did not label with FITC-anti-AQP1 IgG. Fluorescence video images of RBCs from two normal, type O donors showed uniform AQP1 distribution on the cell surface. The lateral diffusion coefficient of AQP1 was $2.7 \pm 0.3 \times 10^{-11}$ cm^2/s, and the fractional mobility was 70 ± 16 %. Anti-human IgG caused lateral immobilization of AQP1 on RBCs previously incubated with FITC-anti-AQP1, but did not cause morphologic clustering or capping. We conclude that AQP1 is laterally mobile in intact human RBC membranes. The lateral diffusion coefficient of AQP1 is similar to that of other integral membrane proteins, such as band 3 and glycophorin A, which exhibit constrained lateral diffusion due to steric interactions with the spectrin-based membrane skeleton.

W-AM-E6

ANALYSIS OF THE AQUAPORIN-1 STRUCTURE BY ELECTRON CRYSTALLOGRAPHY, INFRARED SPECTROSCOPY, AND ATOMIC FORCE MICROSCOPY ((T.Walz[1], D. Typke[2], B.L. Smith[3], V. Cabiaux[4], D.J. Müller[1], P. Agre[3], and A. Engel[1])) [1]Maurice E. Müller-Institute, Biozentrum, CH-4056 Basel, Switzerland; [2]Max-Planck-Institut für Biochemie, D-8033 Martinsried, Germany; [3]Johns Hopkins Univ. School of Medicine, Baltimore, MD 21205-2185, USA; [4]Laboratoire de Chimie Physique des Macromolécules aux Interfaces, Université Libre de Bruxelles, Belgium. (Spon. by E. Lattman)

Aquaporin-1 tetramers were reconstituted into 2-D crystals and analyzed by cryo-electron microscopy, attenuated total reflection Fourier transform infrared spectroscopy, and atomic force microscopy. The water channel protein exhibits an α-helix content of 60% with α-helices largely oriented perpendicular to the membrane. The 6 Å projection map of glucose embedded samples recorded at -170° C reveals eight density maxima, seven of which are located at the periphery of the molecule. The surface topography recorded with the atomic force microscope confirms the asymmetry of the tetramer with respect to the membrane previously established by negative stain electron microscopy. Future studies should resolve the physical structure of AQP1 with that deduced from molecular genetic studies, establish the functional domains of AQP1, and elucidate the structures of other members of the aquaporin family.

W-AM-E7

EVIDENCE FOR COUPLING OF THE CHLORIDE CHANNEL AND ATPASE ACTIVITIES OF PURIFIED CFTR
Li, C., Ramjeesingh, M., Wang, W., Hewryk, M. and Bear, C.E. Division of Cell Biology, Research Institute, Hospital for Sick Children, 555 University Ave. Toronto, CAN. (Spon. by S. Grinstein)

The Cystic Fibrosis Transmembrane Conductance Regulator (CFTR) possesses two putative nucleotide binding folds (NBFs) and a novel regulatory domain (R domain). Activity of CFTR as a chloride channel requires PKA- mediated phosphorylation of the R domain as well as nucleotide binding and hydrolysis at one or both NBF's. Plausible models for the role for ATP hydrolysis in CFTR channel activity have been formulated on the basis of electrophysiological studies in cardiac cells and recombinant cell expression systems. However, direct biochemical evidence supporting a role for ATP hydrolysis in channel gating is lacking. In our present studies, we show that the intact, unphosphorylated purified protein possesses weak intrinsic ATPase activity (apparent K_M= 789 μM, Vmax= 50 nmol/min/mgm protein). We suggest that the intrinsic ATPase activity of CFTR is coupled with CFTR channel gating as both functions are stimulated by PKA phosphorylation (ATPase activity is enhanced two to three fold), both functions require Mg^{2+}, assessed as sensitivity to EDTA (10 mM) and both activities are inhibited by sodium azide (1 mM).
These findings support the hypothesis that ATP hydrolysis is required for CFTR channel gating and provides insight into the mechanism of action of this protein.
This project was funded by the CCFF, MRC and NIH

W-AM-E8

STABLE SUB-CONDUCTANCE STATES OF CFTR CHLORIDE CHANNELS. ((F. Wang, I. C.-H. Yang, E.M. Price* and T.-C. Hwang)) Departments of Physiology and *Veterinary Biomedical Sciences, Dalton Cardiovascular Research Center, University of Missouri, Columbia, MO 65211. (Spon. by V. Huxley)

The reported single-channel conductance for CFTR Cl channels is about 10 pS. In addition to this predominant 10 pS conductance state, we observed at least two stable sub-conductance states (2.4 ± 0.2 pS, n=65 and 6.4 ± 0.2 pS, n=51) in both Hi-5 insect cells expressing recombinant CFTR, as well as in Calu-3 cells which express endogenous CFTR. In cell-attatched patches, the regulation mechanisms of both full conductance and sub-conductance channels are the same; channels are activated by forskolin and genistein and calyculin A are both enhanced in forskolin-induced sub-conductance channels. Most importantly, in excised patches, the activities of sub-conductance states are ATP-dependent, a unique property of CFTR Cl channels. Dwell time analysis of patches containing a single channel reveals similar gating kinetics between full conductance and one of the sub-conductance states (the one with 2.4 ± 0.2 pS): τ_{open} ~ 0.32 s, τ_{close} ~ 0.51 s for sub-conductance state and τ_{open} ~ 0.34 s, τ_{close} ~ 0.52 s for full conductance CFTR. In a patch containing all these conductance states, spontaneous conversions from high conductance to low conductance were frequently observed. Relative open time distributions for sub-conductance states and full conductance CFTR are almost time independent, suggesting inter-conversions between sub-conductance states and full conductance CFTR. We thus conclude from the above results that CFTR can assume different conductance states. Supported by the AHA, Missouri Affiliate, and MU Molecular Biology Program.

W-AM-E9

INCREASING INTRALUMINAL [Ca^{2+}] INHIBITS THE Ca PUMP OF BRAIN MICROSOMES. ((K.M. Nutt and R.F. Abercrombie)) Department of Physiology, Emory University School of Medicine, Atlanta, GA, 30322.

In rat brain microsomes, ER Ca^{2+} load significantly influenced the rate of ATP-dependent Ca^{2+} uptake as well as the time constant of basal Ca^{2+} efflux. For uptake experiments, microsomes were pre-loaded with solutions of 0, 10, or 25 μM Ca^{2+} and then exposed to a 25 μM free Ca^{2+} solution containing tracer $^{45}Ca^{2+}$. The initial Ca uptake rates were 0.048, 0.018, and 0.013 $\mu mol \cdot g^{-1} \cdot s^{-1}$ and the time constants (time to reach 63% of steady-state Ca accumulation) were 53, 129, and 141 s, respectively. For efflux experiments, $^{45}Ca^{2+}$ fractions were collected while passing, at a constant flow rate, a Ca-free buffer solution over microsomes that had been pre-loaded with either ≤0.5 μM free Ca^{2+} ("unloaded") or 25 μM free Ca^{2+} ("pre-loaded"). The time constant of efflux was significantly higher for the "unloaded" versus the "preloaded" microsomes: 491±43 and 286±15 s, respectively. Because increased loadedness decreased the time constant of basal Ca efflux, the increase in the time constant of uptake can be explained by increasing inhibition of the ER Ca pump during the time course of accumulation, as intraluminal [Ca^{2+}] rises. Supported by NIH NS-19194.

W-AM-F1

CALCIUM BLOCK OF A NOVEL ATP-GATED ION CHANNEL EXPRESSED IN SPINAL CORD AND IMMUNE CELLS. ((A. Surprenant, E. Kawashima, F. Rassendren and G. Buell)) Glaxo Institute for Molecular Biology, Geneva, Switzerland CH 1228. (Spon. by W. Almers)

The P_{2X} family of receptors have presented a new molecular architecture for ligand-gated ion channels: they have two membrane-spanning domains, relatively short intracellular N and C termini and a large, cysteine-rich extracellular loop. Six P_{2X} receptor cDNAs have been isolated previously; they show 34 - 46% homology with each other and all encode ATP-gated cationic channels which also have a significant calcium permeability (about 4:1 calcium:sodium). We now have isolated a 7th member of this family; it encodes a 595 aa protein with the same structural motif as the others except for a very long intracellular C-terminus. Northern blot analysis shows strong expression in macrophage, lymphocyte, microglia and spinal cord. Expression of this cDNA in HEK cells reveals an ATP-gated ion channel whose monovalent cationic permeability is very similar to other P_{2X} receptors but which appears to exhibit a much higher calcium permeability (~25:1 over sodium). Unlike the other P_{2X} receptors, this ion channel is also strongly blocked by extracellular calcium (half-maximum block at 0.7 mM). The calcium block is voltage independent and is not overcome by increasing concentrations of ATP or other P_{2X} receptor agonists.

W-AM-F2

$P_{2x}\alpha4$: AN ATP-ACTIVATED IONOTROPIC RECEPTOR CLONED FROM RAT AND HUMAN BRAIN. ((W. Stühmer, F. Soto, J.M. Gómez-Hernández, M. Hollmann[1], C. Karschin and M. García-Guzmán)) Molecular Biology of Neuronal Signals and [1] Glutamate Receptor Lab., Max-Planck Institute for experimental Medicine, Hermann-Rein-Str. 3, D-37075 Göttingen, Germany.

We have isolated a cDNA encoding an ATP-activated ionotropic receptor from rat and its human analogue. The cDNA codes for 388 aa with a proposed topology of 2 transmembrane domains, most of the protein being extracellular. The primary sequence shows homology to previously cloned ATP ionotropic receptors (44 - 50 %). Expression in *Xenopus* oocytes gives a fast ATP-activated inward current that desensitizes in the presence of the agonist. The $P_{2x}\alpha4$ receptor is activated by nucleotide analogues in the following order of efficacy (100 μM): ATP>>2MeSATP≥ CTP>α,β-MeATP>dATP. The sensitivity to ATP (IC_{50} = 7 μM) is enhanced by Zn^{2+} in a concentration-dependent manner. The channel is equally permeable to Na^+ and K^+ and exhibits a high Ca^{2+} permeability. *In situ* hybridization reveals the expression of $P_{2x}\alpha4$ mRNA in CNS neurones. Northern blot and RT-PCR analysis demonstrate a wide distribution in various tissues, including blood vessels and leukocytes. This suggest that $P_{2x}\alpha4$ may mediate ATP-dependent biological responses in a variety of different cell types.

W-AM-F3

MOLECULAR DETERMINANTS OF AGONIST AND ANTAGONIST ACTION ON CYCLIC NUCLEOTIDE-GATED CHANNELS (PART TWO) (RH Kramer) Dept. of Molec. & Cell. Pharmacol., Univ. of Miami, Miami, FL 33101

Photoreceptor (RET) and olfactory (OLF) cyclic nucleotide-gated (CNG) channels are activated by a process involving ligand binding and channel opening. Last year we showed that specific phosphorothioate derivatives of cAMP and cGMP (Rp-cAMPS and Rp-cGMPS) *can* antagonize CNG channel activation, but they act differently on the two channels. For example Rp-cGMPS is an agonist of RET and an antagonist of OLF channels. Hence, while both bind Rp-cGMPS, only RET channels couple binding to gating. To identify the protein region that determines whether ligand binding is coupled to gating we generated chimeras between RET and OLF channels. These experiments localized the region to a 125 amino acid putative cyclic nucleotide binding domain (CNBD) in the carboxyl terminus. Homologous CNBD's are comprised of a β-barrel structure that primarily interacts with the phosphoribose moeity of cyclic nucleotides and an α-helix that primarily interacts with the purine. Substituting either the β-barrel or the α-helix from OLF into RET converts Rp-cGMPS from agonist to antagonist. The α-helix chimera also has a reduced sensitivity to cGMP, suggesting that a general change in the free energy of channel opening contributes to the change in the response to Rp-cGMPS. In contrast, the response to Rp-cGMPS is selectively changed in the β-barrel chimera, with no change in cGMP sensitivity. Thus the β-barrel contains a region that specifically couples binding of Rp-cGMPS to gating of the channel. We have recently identified specific amino acids that account for the effects of these chimeras. Supported by NIH grant NS30695.

W-AM-F4

MECHANISM OF POTENTIATION OF ROD CYCLIC NUCLEOTIDE GATED CHANNELS BY PROTONS ((S.E. Gordon and W.N. Zagotta)) Howard Hughes Medical Institute, Univ. of Washington, Box 357370, Seattle, WA 98195-7370.

We have examined the effects of intracellular protons on CNG channels from bovine rod photoreceptors expressed in Xenopus oocytes. We characterized two components of potentiation by protons. One component potentiated cGMP-bound and cAMP-bound channels to the same extent, while another potentiated only cAMP-bound channels. Both components of potentiation could be described by a mechanism in which protons bound primarily to the channel open configuration. The potentiation specific to cAMP-bound channels could be accounted for by protonation of aspartic acid 604 (D604). An unfavorable electrostatic interaction between the carboxylate of D604 and the purine ring of cAMP was postulated to account for the normally poor activation of the channels by cAMP. Protonation at this site removed the unfavorable interaction, and allowed cAMP to act as nearly a full agonist. The nucleotide-nonspecific potentiation resulted partially from protonation of H468. Experiments with subunit 2 of the rod CNG channel, which lacks both protonatable sites, explain the reduced efficacy of protons reported for native channels.

W-AM-F5

ACTIVATION OF CYCLIC NUCLEOTIDE-GATED CHANNELS EXAMINED BY TANDEM LINKAGE OF SUBUNITS. ((M. D. Varnum and W. N. Zagotta)) Dept. of Physiology and Biophysics and Howard Hughes Medical Institute, Univ. of Washington, Seattle, WA 98195.

Cyclic nucleotide-gated (CNG) ion channels of retinal photoreceptors and olfactory neurons are multimeric proteins of unknown stochiometry. We have previously demonstrated that mutation of a single aspartic acid residue (D604) in the binding domain of the bovine rod CNG channel can profoundly alter agonist discrimination, converting a cGMP-selective channel to one that exhibits cAMP selectivity. This resulted from an alteration in the relative ability of these agonists to promote the allosteric conformational change(s) associated with channel activation, not from a modification of initial binding affinity. In order to investigate the molecular mechanisms underlying CNG channel activation, we have used tandem cDNA constructs of the rod CNG channel to generate heteromultimeric channels composed of wild-type and mutant subunits, using specific point mutations that affect channel acitvation. At saturating concentrations of agonist, the behavior of channels comprised of mixtures of mutant and wild-type subunits was consistent with a model for channel activation involving a concerted conformational change in all of the channel subunits. Similar behavior of the reciprocal heterodimers implies that the channel stochiometry is some multiple of two, and is consistent with a tetrameric quaternary structure for the functional channel complex. Steady-state dose-response relations for homomultimeric and heteromultimeric channels were well fit by a Monod, Wyman and Changeux model for a concerted conformational transition stabilized by binding of agonist.

W-AM-F6

SUBUNIT 2 ALTERS LIGAND SPECIFICITY OF ROD CNG CHANNELS. ((A.A. Fodor and W.N. Zagotta)) Dept. of Physiology and Biophysics and Howard Hughes Medical Institute, Univ. of Washington, Seattle, WA 98195.

The cGMP-gated channel from mammalian retinal rods closes in response to a fall in cGMP concentration brought about via the signal transduction cascade initiated by photon absorption. We compared the potency of cAMP as an agonist for channels formed either from subunits 1 and 2 or formed from subunit 1 alone. Using patch-clamp recordings from channels expressed in Xenopus oocytes, we found that cAMP was a significantly more effective agonist for channels formed from subunits 1 and 2 than for channels formed from only subunit 1. Native channels, which are formed from both subunits, have been shown to have a higher efficacy for cAMP then do expressed channels formed from only subunit 1. Our results suggest that subunit 2 makes the channels more sensitive to cAMP. Subunits 1 and 2 have approximately a 30% overall sequence identity, but most of the residues in the cyclic-nucleotide binding pocket are either identical or conserved. The two subunits differ, however, at a residue in the binding pocket (equivalent to D604 in subunit 1) which has been shown to be important in cyclic-nucleotide discrimination. This suggests that the difference at this residue may explain why cAMP is a better agonist for channels formed from both subunits then it is for channels formed only from subunit 1.

W-AM-F7

GATING AND PERMEATION THROUGH THE CYCLIC GMP-GATED CHANNEL OF VERTEBRATE RODS ARE TIGHTLY COUPLED. ((G. Bucossi*, E. Eismann#, F. Sesti#, M. Nizzari*, M. Seri°, U.B. Kaupp#, V. Torre+*)) * I.N.F.M., Genova, Italy, # Forschungszentrum Jülich, Jülich, Germany, °Ospedale Gaslini, Genova, Italy and + Dipartimento di Fisica, Universita' di Genova, Genova, Italy.

When glutamate 363 of the alpha subunit of the cGMP-gated channel from vertebrate rods was mutated to asparagine, serine or alanine, the current activated by a steady cGMP concentration declined with time in mutant channels. No current decline was observed when threonine 359, 360 and 364 were mutated to alanine or when other charged residues in the pore region were neutralized. The amount of current decline and its time course were significantly voltage dependent. The current decline in mutants E363A, E363S and E363N was only moderately dependent on the cGMP concentration (from 10 to 1000μM) and was not caused by a reduced affinity of the mutant channels for cGMP. Analysis of current fluctuations at a single-channel level indicated that current decline was primarily caused by a decrease of the open probability. The w.t. channel was not permeable to dimethylammonium or triethylammonium. When glutamate 363 was replaced by a smaller residue such as alanine or glycine, mutant channels became permeable to these large organic cations. These results suggest that gating and permeation through the cGMP-gated channel from bovine rods are intrinsically coupled.

W-AM-F8

THE CYCLIC GMP-GATED CHANNEL FROM VERTEBRATE RODS HAS MULTIPLE OPEN STATES. ((G. Bucossi*, E. Eismann#, F. Sesti#, M. Nizzari*, M. Seri°, U.B. Kaupp#, V. Torre+*)) * I.N.F.M., Genova, Italy, # Forschungszentrum Jülich, Jülich, Germany, °Ospedale Gaslini, Genova, Italy and + Dipartimento di Fisica, Universita' di Genova, Genova, Italy.

When the alpha subunit of the cGMP-gated channel from vertebrate rods is heterologously expressed in *Xenopus laevis* oocytes, cGMP-gated channels with a single channel conductance of about 27 pS are observed. When glutamate in position 363 is substituted by an aspartate, the mutant channel E363D has an additional open state with a conductance of about 48 pS. The mutant channel T364M appears to have three open states, with conductances of about 18, 28 and 43 pS as in the cGMP-gated channel from olfactory neurons of the catfish (Root & MacKinnon, Science, 265, 1852-1856, 1994). The multiple open states observed in mutant channels E363D and T364M are independent from the cGMP concentration and are much less visible at positive membrane voltages. Increasing the proton concentration in the extracellular and\or intracellular medium decreases the conductance of these open states. These results indicate that the cGMP-gated channel from vertebrate rods has several open states, with a similar conductance of about 27 pS in the w.t. channel. In the presence of perturbations of the molecular structure in the pore region these open states have distinguishable conductances and can be clearly separated.

ATOMIC FORCE MICROSCOPY

W-AM-G1

PROBING ACTIN-MYOSIN INTERACTIONS WITH THE ATOMIC FORCE MICROSCOPE. ((John P. Santos and Jeffrey G. Forbes)) Department of Chemistry and Biochemistry, University of Maryland, College Park, MD 20742-2021.

Actin and myosin account for about two-thirds of the protein in myofibrils and are responsible for motility and force generation in these structures. *In vivo* these two proteins usually exist as filamentous structures. However, actin may be induced to form other structures *in vitro* by manipulation of the solution conditions used for polymerizing G-actin. In the absence of magnesium and in presence of different lanthanide ions, actin will polymerize into tubes or sheets. While these non-filamentous structures have not been observed *in vivo*, they provide a means for studying actin-actin interactions different from those present in actin filaments. In actin sheets and tubes, a larger portion of the actin monomer's surface is presented to the environment than in filaments. Atomic force microscopy data will be presented on the different forms of polymerized actin and their interactions with myosin.

W-AM-G2

A NOVEL METHOD FOR MEASURING THE INTERACTION FORCE BETWEEN THE β_2-ADRENERGIC RECEPTOR AND ITS AGONIST ALPRONOLOL. ((Shaohua Xu and Morton F. Arnsdorf)) University of Chicago, Chicago,Il 60637. shxu@medicine.bsd.uchicago.edu. (Spon. by S. Shroff)

A new method is described for the detection of the interaction force between the β_2-adrenergic receptor (BAR) and the agonist alprenolol (AP). The scanning (atomic) force microscope (SFM) was used to monitor the inter-molecular interaction forces. We found that the SFM tip could be coated with amphipathic molecules including membrane lipids. The BARs reconstituted in phosphatidylcholine (PC) vesicles were coated onto the SFM tip. A rupture force (adhesion force) was measured for separating the receptor coated tip and the AP-sepharose bead in the absence of free AP (1.06nN ± 0.54, n=100). The force decreased by 50% in the presence of 25 nM of free AP (0.52nN ± 0.26, n=100) and disappeared in the presence of 25 μM of free AP. The experiment was performed in Tris buffer (100 mM NaCl, 10 mM Tris·HCl, 2 mM EDTA, pH 7.2). The frequency of the occurrence of the rupture force was found dependent on the molar ratio of the BARs to the lipids, decreased if less BARs were present in the same amount of lipids. The rupture force was not observed if the BARs reconstituted in the PC vesicles were thermally denatured before coated onto the tip. The SFM tip coated with PC lipids with no BARs showed no rupture force. The coating of the SFM tip with amphipathic lipid molecules was stable over hours. Coating the tip with charged lipid molecules has allowed SFM to be used as an electrostatic force microscope (EFM, or an electrostatic sensor) to monitor surface charges in aqueous solutions (Shaohua Xu and Morton F. Arnsdorf, Proc. Natl. Acad. Sci. USA, 92(22), 10384-10388, 1995). The EFM and the biospecifically functionalized SFM should have broad applications in the study of surface charges and ligand (hormones, drugs, etc)-receptor interactions.

W-AM-G3

CRYO ATOMIC FORCE MICROSCOPY: OPPORTUNITIES AND PROBLEMS. ((Zhifeng Shao, Yiyi Zhang, Jun Sheng and Jianxun Mou)) Department of Molecular Physiology & Biological Physics, University of Virginia, Box 449, Charlottesville, VA 22908. (Sponsored by NIH and NSF)

One of the major limitations in high resolution biological atomic force microscopy (AFM) is the softness of most hydrated biological materials[1]. To overcome this problem, cryogenic AFM can be an effective approach[2,3]. We have recently shown that an AFM operated in liquid nitrogen vapor is more appropriate than other approaches, because the problem of surface contamination can be entirely eliminated[4]. Direct measurements on individual macromolecules demonstrate that the molecular rigidity is greatly improved at cryogenic temperatures, providing a solid basis for the validity and future development of biological cryo-AFM. Applications of this cryo-AFM to a large number of biological specimens indicate that, even at this early stage of development, the cryo-AFM is already capable of imaging structures, at nm resolution, that were too flexible for room temperature AFM. This reoslution is higher than conventional SEM and comparable to normal TEM. We will discuss several examples, including IgA, α_2M, and red cell membranes of which interesting new observations have been made. We will also discuss other unique applications of the cryo-AFM in biology, when deep etch and freeze fracture are fully incorporated into this system. Sub-nm resolution should be achievable when the methodology is further improved.

References: [1]Z. Shao & J. Yang, *Q. Rev. Biophys.* 28:195(1995). [2]C.B. Prater et al., *J. Vac. Sci. Technol.* B9:989(1991). [3]J. Mou et al., *Rev. Sci. Instrum.* 64:1483(1993). [4]W. Han et al., *Biochemistry.* 34:8215(1995).

W-AM-G4

TOPOGRAPHY OF SUPPORTED PHOSPHOLIPID BILAYERS AND POTENTIAL CONTRAST OF PORES IMAGED BY ATOMIC FORCE MICROSCOPY. ((M. Beckmann[1], C. Böhm[2], P. Nollert[3] and H.-A. Kolb[4])) [1] Becton Dickinson, Tullastr. 8-12, D-69126 Heidelberg. [2] Gesamthochschule Duisburg, Fachbereich Elektrotechnik, Bismarckstr. 81, D-47048 Duisburg. [3] Max-Planck-Institut für Biologie, Abt. Membranbiochemie, Corrensstr. 38, D-72076 Tübingen. [4] Institut für Biophysik, Universität Hannover, Herrenhäuserstr. 2, D-30419 Hannover.

Supported unilamellar planar bilayers of 1,2-dipentadecanoyl-*sn*-glycero-3-phosphatidylcholine (diC15-PC) were prepared by vesicle fusion on freshly cleaved mica or silicon wafers. The topography of the bilayer surface was imaged in a fluid cell by an atomic force microscope (TMX2000) under electrolyte solution. From high resolution images the pattern of single lipid molecules could be resolved in the gel phase. A mean surface area per molecule of about 43 $Å^2$ was obtained. The two-dimensional pattern showed no higher degree of order. Consecutive scanning of supported bilayers on mica or silicon wafer induced parallel rows of lipid molecules with a spacing of 0.68 nm. This molecular arrangement was interpreted as scanning induced Schallamach waves. Bilayer with defects were formed which allowed the measurement of their thickness (about 4.8 nm). The slope of the induced troughs and valleys decreased by consecutive scanning. The pattern of the surface did not vary if the bilayer was formed of diC16-PC. The lipid bilayer could be dissolved by superfusion with DMSO containing electrolyte solution until the pure mica surface remained. Images of the different phases of dissolution could be recorded. Potential contrast and topography of track-etched mica could be simultaneously recorded by a modified atomic force microscope in the layered imaging mode. The membranes contained pores with diameters of up to 300 nm. Under electrolyte solution a comparison of the potential contrast and the topography showed a similarity in the structure, but significant differences in the range of the pores. The method offers the possibility to study simultaneously the topography of membrane surfaces and the location of conducting pores in the nanometer scale.

W-AM-G5

THE PHYSICAL MECHANISM OF THE CLOSE-PACKING OF MEMBRANE-BOUND DNA IN SOLUTION ((Jie Yang[1], Lijiang Wang[2] and R. Daniel Camerini-Otero[2])) [1]Department of Physics, University of Vermont, Cook Building, Burlington, VT 05405 and [2]Genetics and Biochemistry Branch, NIDDK, NIH, Bethesda, MD 20892-1810.

By preparing supported cationic lipid bilayers in physiologically relevant solutions, we have established that the pitch of membrane-bound DNA can be directly visualized with the atomic force microscopy, that the pitch has a wide distribution for both linear and circular double strand DNAs, and that the binding of DNA to the cationic lipid bilayer is surprisingly strong, with a lower limit of about 5 kcal/mol per helical turn. It is also found that membrane-bound DNA molecules attract each other strongly, resulting in their close-packing on the bilayer. To investigate the physical mechanism of this close-packing, we carried out structural studies of membrane-binding of double and single stranded oligonucleotides, various DNA molecules, and mixtures of several of them on supported cationic lipid membranes under various binding conditions. Our results indicate that this attraction is strongly dependent on the phase state of the hosting lipid bilayers, and suggest that the hydrophobic interaction between lipid molecules is responsible for the close-packing of membrane-bound DNA molecules. Details of experimental conditions, and characterization of the method will also be presented.

W-AM-G6

AFM IMAGING OF DNA AND OTHER BIOLOGICAL MOLECULES: USE OF SILYLATED MICA. ((Y. L. Lyubchenko[1,2*], A. A. Gall[3], L. S. Shlyakhtenko[1,2] and S. M Lindsay[2])). Department of [1]Microbiology and [2]Physics, Arizona State University, Tempe, AZ 85287-2701 and [3]MicroProbe Corp., 1725 220th St. SE, #104, Bothell, WA 98021.

Progress towards rapid and simple characterization of biomolecular samples by scanning probe microscopy is impeded mainly by limitations of the sample preparation methods. We have earlier suggested a simple approach, based on treatment of mica with aminopropyltriethoxy silane (APTES). This makes the surface positively charged (AP-mica) and able to hold DNA in place for imaging. The AP-mica is an appropriate substrate for numerous nucleoprotein complexes as well as allowing the AFM imaging *in situ* in the buffer solutions. We are developing this approach for fixing molecules for making negatively charged substrates and substrates with patterned charge distributions, as well as hydrophobic substrates. Methylated mica surface (Me-mica) allowed us to get AFM images of hydrophobic antenna complexes isolated from green photosynthetic bacteria. Me-mica may be converted into charged substrates after the treatment with water solutions of organic salts and ionic detergents. These activated positively charged surfaces show high activity towards binding DNA molecules. Applications of functionalized mica substrates for other types of microscopies will be discussed.

W-AM-G7

AFM STUDIES OF PROTEIN-INDUCED DNA LOOPING. ((Y. L. Lyubchenko[1], T. Aki[2], H.E. Choy[2] and S. Adhya[2])). [1]Department of Microbiology, Arizona State University, Tempe, AZ 85287-2701 and [2]Laboratory of Molecular Biology, NCI, NIH, Bethesda, MD 20892.

DNA looping is generated by a protein or complex of proteins that binds to two distant sites on a DNA molecule. This seemingly simple phenomenon appears to be a ubiquitous regulatory mechanism for all genetic processes in prokaryotes and eukaryotes. We have studied the loop formation effect induced by Lac and Gal repressors after their binding to O_E and O_I operator regions. In addition to DNA molecules carrying the wild-type *gal* operon region which is chracterized by 114 bp separation between operators O_E and O_I, plasimd DNA molecules containing incertions of 50, 300 and 500 bp have been studied. Complexes of repressors were prepared for linear and supercoiled DNA molecules, deposited onto AP-mica and after drying imaged with AFM. The role of the DNA topology in the protein-induced looping effect will be discussed.

W-AM-G8

DNA ON CATIONIC LIPID BILAYERS FOR AFM IMAGING IN SOLUTION: RESOLUTION OF THE DOUBLE HELIX. ((D.M. Czajkowsky, J. Mou, Y.-y. Zhang and Z. Shao)) Department of Molecular Physiology & Biological Physics, University of Virginia, Box 449, Charlottesville, VA 22908. (Sponsored by NIH and NSF)

AFM has been shown to be a powerful imaging method for the study of DNA structures, in addition to other biological samples[1-3]. In spite of the many methods hitherto developed, the resolution of AFM on dsDNA has been limited to several nm both in solution and in air[4-6]. Although the probe force and size are certainly important limiting factors for AFM imaging[1,2], it is not clear that these are responsible for the low resolution of DNA. We have recently introduced supported cationic lipid bilayers as a substrate for adsorbing DNA[7]. Since at neutral pH the cationic lipids are positively charged and DNA is negatively charged, the electrostatic interaction resulted in well adsorbed and well ordered DNA specimens. In buffers containing EDTA and Tris, we show that such samples are very stable, and individual plasmids can be resolved with excellent reproducibility. Upon heating, closely packed samples can be prepared, and the pitch and handedness of the double helix are clearly resolved. This is the highest resolution ever achieved of DNA with any direct imaging technique.

References: [1]C. Bustamante et al., *Curr. Opin. Struct. Biol.* 4:750(1994). [2]H.G. Hansma and J. Hoh, *Annu. Rev. Biophys. Biomol. Struct.* 23:115(1994). [3]Z. Shao & J. Yang, *Q. Rev. Biophys.* 28:195(1995). [4]J. Yang et al., *FEBS Lett.* 301:173(1992). [5]C. Bustamante et al., *Biochemistry* 31:22(1992). [6]H.G. Hansma et al., *Science* 256:1180(1992). [7]J. Mou et al., *FEBS Lett.* 371:279(1995).

SCANNING PROBE MICROSCOPIES

W-AM-SymII-1

NON-LINEAR OPTICAL MICROSCOPY. ((Watt W. Webb)) Applied and Engineering Physics, and Developmental Resource for Biophysical Imaging and Opto-electronics (DRBIO), Cornell University, Ithaca, NY 14853.

Non-linear laser microscopy based on multi-photon molecular excitation is reaching a user-friendly maturity that offers a powerful tool for cellular and molecular biophysics. Intrinsically 3-d resolved microscopy for fluorescence imaging, photochemical micropharmacology and measurements of molecular dynamics are provided with minimal photodamage in living cells by simultaneous absorption of two or more red/infrared photons from the 100 MHz train of 100fs pulses of mode locked lasers. Three photon excitation can provide convenient red light detectability and assay of amino acids, and polypeptide hormones and neurotransmitters that absorb below 350nm. Two photon excitation spectra often show their largest cross sections at wavelengths far shorter than twice the one photon absorption peaks thus providing convenient red light excitation of many of the familiar blue and green absorbing dyes as well as UV absorbing fluorophores. Our extensive three-photon and two photon excitation cross section data are becoming available, and physical theory of multi-photon excitation guides experimental design. Recent developments include sensitivity to detect single fluorophores in solution at picoMolar concentrations, submicron 3-d resolved Ca activity ratio images, neurotransmitter release by cage activation, and numerous applications of multicolor fluorescent indicators and deep tissue fluorescence imaging. Supported at DRBIO by NIH (RR04224 and RR07719) and NSF (BIR 9419978)

W-AM-SymII-2

TIME-RESOLVED SPECTROSCOPY OF SINGLE MOLECULES. ((J. K. Trautman and J. J. Macklin)) AT&T Bell Labs, 600 Mountain Ave., Murray Hill, NJ 07974.

Room-temperature spectra and excited state lifetimes of single molecules obtained with both near-field and conventional, far-field optics will be presented. Superior spatial resolution is available with near-field excitation, whereas presently, excited state lifetimes can be accurately determined only under far-field illumination. In addition, greater data rates are possible with far-field excitation, without perturbing the molecule. Which method proves better will depend on the particulars of the system under investigation. In detailed experiments, we have elucidated the correlations among the orientation, the spectral shift and the excited state lifetime of molecules at a dielectric interface. In dynamic studies, the intersystem crossing and isomerization rates have been determined on a molecule-by-molecule basis. Further results on model systems and those resulting from our first attempts to apply these methods to biological samples will also be presented.

W-AM-SymII-3

AFM--THE ART OF TOUCHING MOLECULES.((H. Gaub))
Technical University of Munich.

W-AM-SymII-4

ANALYSIS OF MEMBRANE PROTEIN STRUCTURE AND FUNCTION BY ATOMIC FORCE AND ELECTRON MICROSCOPY. ((T. Walz, D.J. Müller, Ch. Henn, G. Tsiotis, and A. Engel)) Maurice E. Müller-Institute for Microscopical Structure Biology at the Biozentrum, Klingelbergstrasse 70, CH-4056 Basel.

In spite of advances in x-ray techniques, and recent developments in NMR spectroscopy, the structure of most membrane proteins remains elusive. As solubilization tends to destabilize the proteins, detergent-solubilized proteins rarely form crystals suitable for x-ray analyses. A powerful alternative is the reconstitution of two dimensional (2D) membrane protein crystals in the presence of lipids. In this approach the native environment of membrane proteins is restored, as well as their biological activity. Cryo-electron microscopy is used to assess the 3D structure of the protein at atomic resolution. On the other hand, the atomic force microscope (AFM) has provided information about the topography of native biological membranes at subnanometer lateral and atomic scale vertical resolution. Furthermore, the AFM has demonstrated its ability to monitor conformational changes of active proteins. Our goal is to crystallize a wide variety of membrane proteins and to exploit the combination of electron microscopy and AFM to elucidate their structure and function.

SYNAPTIC TRANSMISSION AND PLASTICITY

W-AM-H1

MODELING THE EFFECTS OF AMBIENT GLUTAMATE ON NMDA AND NON-NMDA SYNAPTIC CONDUCTANCES AND CELL EXCITABILITY. ((W.R. Holmes)) Department of Biological Sciences, Ohio University, Athens, OH 45701.

Models were used to study the effect of ambient glutamate on NMDA and non-NMDA synaptic conductances and cell excitability in a dentate granule cell. Equations for NMDA and non-NMDA binding reactions were used in conjunction with a diffusion model of the synaptic cleft and the volume outside the cleft to compute NMDA and non-NMDA conductances at a synapse for a range of ambient glutamate concentrations. The computed conductances were used in a model of a hippocampal dentate granule cell to estimate the effects of ambient glutamate on cell excitability. For an ambient glutamate concentration of 2.9 μM, 20% of non-NMDA receptors and 94% of the NMDA receptors were desensitized. This high rate of desensitization meant that the peak number of NMDA receptor channels opened at a synapse by release of a vesicle of glutamate was, on average, much less than one. Despite this high rate of desensitization, tonically activated channels were responsible for depolarizing the cell by more than 10 mV. Tonic conductances also caused the input resistance and the time constant, τ_0, to be almost two-fold higher at −62 mV than at −85 mV. These effects of ambient glutamate on cell excitability can lead to significant errors in experimental estimates of the time course of the NMDA and non-NMDA components of the EPSP, particularly in experiments in which NMDA blockers are used. If ambient glutamate in the synaptic cleft is 1-3 μM, then the changes in cell excitability predicted by these simulations should be detectable experimentally.
(Supported by NIH grant MH51081).

W-AM-H2

ACTION POTENTIAL-EVOKED CALCIUM TRANSIENTS IN INDIVIDUAL NEOCORTICAL PRESYNAPTIC TERMINALS MEASURED USING TWO-PHOTON FLUORESCENCE SCANNING MICROSCOPY. ((K. Svoboda, D.W. Tank, and W. Denk)) Biological Computation Research Dept., AT&T Bell Laboratories, Murray Hill, NJ 07974.

Synaptic vesicle release is triggered by calcium influx into presynaptic terminals. Fluctuations in calcium influx due to variability in calcium channel activation or action potential (AP) failures could therefore contribute to stochasticity in synaptic transmission. We measured AP-evoked calcium transients in single presynaptic terminals using two-photon fluorescence microscopy. Neocortical brain slices were prepared from 2-3 weeks old rats. Layer 5 or layer 2/3 pyramidal cells, 50 - 100 μm below the slice surface, were voltage clamped using whole-cell tight-seal techniques at 22-24° C. The pipette solution contained 100 μM Calcium Green. Axons and their collaterals displayed numerous varicosities, presumably *en passant* presynaptic terminals. We measured Calcium Green fluorescence in such varicosities with 2 ms temporal resolution in line-scan mode. Fluorescence changes ($\Delta F/F$) evoked with single APs were in the range 20 - 100 %. Fluorescence changes between varicosities were generally smaller. The fluorescence time-course in varicosities was characterized by a fast rise time (as short as ~ 2 ms) and a slow decay time (> 300 ms). The AP-evoked calcium influx varied little, with no apparent failures. Using pairs of APs, we also tested the reliability of calcium influx at very short AP intervals. Even for intervals as short as 10 ms the second AP always led to additional calcium influx of comparable magnitude. It therefore appears that in neocortical pyramidal cells even closely spaced APs reliably invade synaptic terminals and trigger calcium influx.

W-AM-H3

DIFFUSIONAL RESISTANCE OF SINGLE DENDRITIC SPINES MEASURED USING TWO-PHOTON PHOTOBLEACHING.
((K. Svoboda, D.W. Tank, and W. Denk)) Biological Computation Research Department, AT&T Bell Laboratories, Murray Hill, NJ 07974.

Dendritic spines are attached to their parent dendrite via a thin neck. Speculation regarding the functional significance of spines has centered on the presumably large diffusional and electrical resistance of the spine neck. We measured the time-course of diffusional exchange between spines and their parent dendrite. CA1 pyramidal cells in slices of rat hippocampus were dialyzed and voltage clamped using whole-cell electrodes containing 200 μM fluorescein dextran (MW = 3 kD) at 22-24° C. Single spine heads were photobleached using two-photon excitation of fluorescence and the fluorescence recovery due to diffusional exchange with the parent dendrite was characterized with two-photon microscopy (line-scan mode, 2 ms temporal resolution). Fluorescence recovered completely with an exponential time course with time constants in the range τ = 20 - 100 ms. Spine heads are therefore diffusionally isolated on this time scale. The time constant of fluorescence recovery by diffusion can be expressed as $\tau = lV_h/AD$, where l and A are the length and cross sectional area of the spine neck respectively, V_h is the spine head volume, and D is the dextran diffusion coefficient. The spine neck resistance is then $R_h = \tau D\rho_i/V_h$. Comparing spine head fluorescence intensity distributions to published em data provided an estimate of V_h. $D = 1.0 \times 10^{-6}$ cm^2/s was measured *in vitro* using photo-release techniques. Using a cytoplasmic resistivity of $\rho_i \sim 250\ \Omega$ cm, we estimate R_n = 30 - 200 MΩ. The spine neck conductance (R_n^{-1} = 5-30 nS) is large compared to unitary synaptic conductances (< 500 pS), implying that the neck does not attenuate synaptic current. We estimate that during synaptic activation the spine head potential is elevated by at most 5 mV with respect to the dendrite.

W-AM-H4

CALCIUM TRANSIENTS IN CEREBELLAR BASKET CELL AXONS AND THEIR TERMINALS. ((I. Llano and C. Caputo)) AG Zelluläre Neurobiologie, Max-Planck-Institut für biophysikalische Chemie, D37077 Göttingen, FRG.

We report measurements of Ca_i changes along the axons of basket cells from cerebellar sagittal slices of 11-14 days old rats. Basket cells were initially identified from their localization in the lower third of the molecular layer of the cerebellar cortex by visual observation under Nomarski optics. Identification was confirmed in dye-filled cells by the characteristic shape of the axon collateral contacting a Purkinje cell soma. The neurons were loaded with Ca-Green 5 N (0.2 mM) via a patch pipette and held at -60 mV. Fluorescence imaging was carried out with a CCD camera (pixel size 0.36 μm for 63X lens) using 70 to 100 ms exposure periods. Depolarizing pulses evoked cadmium-sensitive fluorescence transients (ΔF) in the cell body, dendrites and axon. Co-localization of ΔF signals in the axonal terminal with Purkinje cell soma was the criterion to distinguish axonal from dendritic processes. ΔF/F transients determined in 3-5 μm^2 regions were larger and decayed faster in the axon and its terminals than in the dendrites and soma. Along the axon ΔF signals were not uniform, being larger in some discrete segments and in the terminals. In these regions, for a 50 ms pulse, ΔF/F increased 3 to 5 fold and decayed with a half time of ~0.5 s.

W-AM-H5

FUNCTIONAL DIVERSITY OF EXCITATORY SYNAPTIC CURRENTS IN CENTRAL NEURONES MEDIATED BY LONG AND SHORT RESIDENCE TIMES OF GLUTAMATE IN THE SYNAPTIC CLEFT ((S. Titz and B.U. Keller)) Zentrum Physiologie, Universität Göttingen, Humboldtallee 23, 37073 Göttingen, Germany.

Glutamate receptor mediated excitatory postsynaptic currents (EPSCs) were recorded in brain stem neurones in the nucleus tractus solitarius by using patch clamp recordings in thin slices. At -60mV glutamate (non - NMDA) receptor mediated EPSCs decayed with time constants around 4ms which was three times slower than decay times found, for example, in cerebellar interneurones (Barbour et al., Neuron, 1994). The slowness of EPSCs in brain stem neurones did not result from dendritic filtering and did not reflect the deactivation kinetics of underlying glutamate receptors (0.7 ms). Instead, data from outside - out patches suggested that slow EPSC decay resulted from the prolonged residence time of glutamate in the synaptic cleft. To investigate the underlying mechanism, EPSCs were recorded in low external calcium concentrations to reduce the probability of synaptic vesicle release. The results suggested that the slowness of EPSCs resulted from the delayed release of neurotransmitter in later phases of the EPSC.

W-AM-H6

NON-STATIONARY NOISE ANALYSIS OF CURRENTS AT PRESYNAPTIC ACTIVE ZONES OF A NEUROMUSCULAR JUNCTION ((D. DiGregorio, B. Yazejian, A. D. Grinnell and J. L. Vergara)) Department of Physiology, UCLA, Los Angeles, CA 90024

Non-stationary noise analysis of whole-cell currents provides an in depth understanding of the stochastic processes involved in the voltage activation of ionic conductances. Using this method, we investigated the gating mechanisms of Ca and Ca-activated-K (K-Ca) channels underlying the initiation of neurotransmitter release in cultured *Xenopus* neuromuscular junctions. We employed perforated whole-cell patch clamp techniques to record presynaptic Ca currents (I_{Ca}) and Ca-activated-K currents ($I_{K\text{-}Ca}$) at the active zone. Average presynaptic current and variance traces were obtained from 60-100 consecutive current records generated with various voltage steps. All presynaptic recordings were obtained from terminals in which postsynaptic currents could be recorded simultaneously. In the presence of TTX and 3,4DAP, predominant $I_{K\text{-}Ca}$ records yielded variance magnitudes of up to 10^3 pA^2. Variance analysis determined the number of open channels to range from 100 - 500, and single channel currents to range from 2 - 10 pA. Charybdotoxin significantly decreased the magnitude of average $I_{K\text{-}Ca}$ and variance traces. By replacing internal K with Cs, isolated average I_{Ca} and variance traces were obtained. I_{Ca} variances reached levels of only up to 10^2 pA^2. Comparative analysis of I_{Ca} and $I_{K\text{-}Ca}$ variance data suggests substantially smaller values for the single Ca channel current and larger number of open Ca channels at the presynaptic terminal. Supported by NIH AR25201.

W-AM-H7

CONGENITAL MYASTHENIC SYNDROME (CMS) CAUSED BY DECREASED AGONIST AFFINITY DUE TO MUTATION IN A LIGAND BINDING DOMAIN OF THE ACETYLCHOLINE RECEPTOR (AChR) ε SUBUNIT. ((K. Ohno, H.-L. Wang, M. Milone, S. Nakano, N. Bren, N.J. Pruitt, A.G. Engel, and S.M. Sine)) Mayo Foundation, Rochester, MN 55905. (Spon. by A. Rich)

In two patients (Pt 1 and 2) with severe CMS partially responsive to cholinesterase inhibitors, end-plate (EP) studies revealed very small EP potentials and currents but normal density of AChRs per EP and on the junctional folds, normal synaptic vesicle size, and intact junctional folds. Single-channel recordings (15 EPs, Pt 2, 12 kHz bandwidth) disclosed a predominant open interval (area: 0.86-1.0 at 1 to 50 μM ACh) with duration about 50% of normal and a minor component with duration close to normal. Mutational analysis in both Pts revealed a heterozygous εP121L substitution plus a heteroallelic null mutation in the ε signal peptide (Pt 1) or in an ε consensus site for glycosylation (Pt 2). Analysis of normal and affected nuclear family members indicate that εP121L plus a null mutation are required to produce disease. Expression studies of εP121L in HEK cells showed reduced binding affinity of ACh for α–ε dimers and $\alpha_2\beta\varepsilon\delta$ pentamers. Single-channel recordings revealed a decreased equilibrium constant for channel opening, from 23 to 0.05, due primarily to a decreased rate of opening. At high ACh concentrations (10-1000 μM), openings showed little or no clustering, indicating a marked resistance to desensitization. P121 is conserved in all subunits of the AChR-related superfamily, and is near residues that contribute to ligand binding affinity (residues 111-117). We hypothesize that εP121L impairs channel opening and desensitization through state-specific decreases in ACh binding affinity.

CARDIAC E-C COUPLING

W-AM-I1

EFFECTS OF PROTEIN PHOSPHATASES 1 AND 2A ON THE $[Ca^{2+}]_i$ TRANSIENT IN RAT VENTRICULAR MYOCYTES. ((W.H. duBell, W.J. Lederer and T.B. Rogers)) Departments of Biological Chemistry and Physiology, University of Maryland School of Medicine, Baltimore MD 21201.

In heart, sarcoplasmic reticulum (SR) Ca^{2+} release is triggered by L-type Ca^{2+} current (I_{Ca}) through a process known as calcium-induced calcium release. Previous studies suggest that the function of the SR Ca^{2+} release channel, or ryanodine receptor (RyR), may be controlled by steady state phosphorylation. To test this, we examined the effects of the serine/threonine phosphatases PP-1 and PP-2A on the voltage dependence of I_{Ca} and the $[Ca^{2+}]_i$ transient. I_{Ca} and $[Ca^{2+}]_i$ transients were measured simultaneously in voltage clamped rat ventricular myocytes with 50 μM indo-1 and PP-1 or PP-2A in the pipette solution (4 units PP activity/ml). I_{Ca}- and $[Ca^{2+}]_i$ transient-voltage relationships were measured between -35 and +63 mV from a holding potential of -40 mV. Between test pulses, cells were held at -60 mV and three conditioning pulses were given from -60 to 0 mV before the cell was ramped to -40 mV for the test pulse. This protocol assured a steady state of SR Ca^{2+} loading. PP-2A had a marked effect on the $[Ca^{2+}]_i$ transient and a lesser effect on I_{Ca}. For example, the $[Ca^{2+}]_i$ transient was decreased by 65% at 0 mV while I_{Ca} was decreased by 19% . Importantly, PP-1 decreased the $[Ca^{2+}]_i$ transient by 43% without decreasing I_{Ca} . Both phosphatases decreased the magnitude of the $[Ca^{2+}]_i$ transient at any given I_{Ca}. These results suggest 1) that there is a steady-state level of RyR phosphorylation that is reversed by PP-1 and 2A and 2) that dephosphorylation decreases the sensitivity of the RyR to triggering by local $[Ca^{2+}]_i$. *(Supported by AHA, MD Affiliate and NIH HL-2 7867)*

W-AM-I2

CALCIUM SPARKS IN MOUSE CARDIOCYTES ORIGINATE AT TERMINAL SR AND REVEAL ANISOTROPY IN CALCIUM DIFFUSION ((Heping Cheng, Rui-Ping Xiao, Harold Spurgeon and Edward G. Lakatta)) LCS, GRC, NIA, NIH, Baltimore, MD 21224

The increasing utilization of transgenic mice in the study of intracellular Ca^{2+} regulation in heart has motivated us to characterize the elementary Ca^{2+} release events or "Ca^{2+} sparks" in mouse cardiocytes. Using confocal microscopy and the fluorescent Ca^{2+} probe, fluo-3, we demonstrate spontaneous ryanodine- and thapasigargin-sensitive local Ca^{2+} release from the SR in adult ventricular cells bathed in 1.4 mM $[Ca^{2+}]_o$. These sparks occur at a rate of 0.74 events /sec /100μm-line scanned, with an amplitude of 206 nM and spatiotemporal dimensions of 53 msec and 2.1 μm (duration and width defined at 50% peak levels). The mouse sparks are thus highly comparable to sparks reported previously in rat and guinea pig myocytes. Importantly, sparks are about 17% wider in longitudinal than in transverse direction, suggesting a microscopic anisotropy of intracellular Ca^{2+} diffusion. This is perhaps due to the organization of mitochondria and myofilaments and may explain an earlier observation that regenerative Ca^{2+} waves propagate faster in the longitudinal direction (Engel et al, *Biophy. J.*, 66:1756, 1994). To delineate the origin of sparks, we use a rhodamine dye to mark extracellular space of the T-tubules (TT) and show that Ca^{2+} sparks are originated at the TT/terminal SR region within a sarcomere. We conclude that Ca^{2+} sparks in mouse myocytes, which are similar to sparks in other species studied, originate at terminal SR and do not spread uniformly. The recording of Ca^{2+} sparks in mouse heart cells will provide us a novel tool to study Ca^{2+} regulation in transgenic mouse models.

W-AM-I3

ROLE OF Ca^{2+}-ACTIVATED Cl^- CURRENTS IN SHAPING THE ACTION POTENTIAL OF CANINE VENTRICULAR MYOCYTES FROM NORMAL AND FAILING HEARTS. ((Brian O'Rourke, Stefan Kääb, David A. Kass, Gordon F. Tomaselli and Eduardo Marban)). Johns Hopkins University, Baltimore, MD 21205.

We have previously shown that the transient outward K^+ current (I_{to}) contributes to the distinct hyperpolarizing "notch" in action potentials of dog ventriculocytes and is down-regulated by tachycardia-induced heart failure. Using extracellular and intracellular solutions designed to mimic physiological conditions (20mM $[Cl^-]_i$, 80μM indo-1 as the only internal Ca^{2+} buffer), we have identified a second component of the transient outward current evident when intracellular Ca^{2+} is minimally buffered. When membrane currents, action potentials and Ca^{2+} transients were recorded at 37°C, a pronounced action potential notch was detected that could only partly be accounted for by I_{to}. In canine cells from both failing and normal hearts, a second transient outward component was identified as a Ca^{2+}-activated Cl^- current ($I_{Cl,Ca}$) by its sensitivity to the chloride channel blocker niflumic acid (10-100μM) and its insensitivity to substitution of Cs^+ for K^+. The size of $I_{Cl,Ca}$ was directly related to the amplitude of the intracellular Ca^{2+} transient: raising external Ca^{2+} from 2 to 10mM or activating β-adrenergic receptors markedly increased $I_{Cl,Ca}$, while blocking Ca^{2+} entry (Cd^{2+}) or SR Ca^{2+} release (ryanodine or caffeine) eliminated the current. All interventions which reduced $I_{Cl,Ca}$ were also capable of decreasing the notch phase of the action potential. Despite maintained peak $[Ca^{2+}]_i$ during a transient, $I_{Cl,Ca}$ deactivated quickly, suggesting a sensitivity to the high $[Ca^{2+}]$ present in the submembrane space during E-C coupling. This was further supported by the lack of $I_{Cl,Ca}$ activation by more slowly rising Ca^{2+} oscillations due to spontaneous SR Ca^{2+} release. Thus, $I_{Cl,Ca}$ makes a significant contribution to the early "notch and dome" contour of the action potential and may partly offset the deficiency of repolarizing K^+ currents during heart failure.

W-AM-I4

The Effect of CaMKII on Cardiac Excitation-Contraction Coupling
((L. Li and D.M. Bers)), Department of Physiology, Loyola Univ. Chicago, Maywood, IL 60153.

The cardiac ryanodine receptor (RyR) can be phosphorylated by calcium-calmodulin dependent protein kinase II (CaMKII) (Whitcher et al., *JBC* 266:11144, 1991) and that phoaphorylation can alter single channel gating properties (Hain et al., *JBC* 270:2074, 1995). We sought to evaluate whether CaMKII modulates EC coupling in intact ferret ventricular myocytes. Using perforated patch clamp we measured whole cell Ca current, SR Ca content (by caffeine application and integration of Na/Ca exchange current) as well as cell contraction. In control conditions the SR was loaded by conditioning pulses and CaMKII could be activated by the elevated $[Ca]_i$. Conditioning pulses were varied such that at the test pulse the SR Ca content was comparable in control and with the CaMKII inhibitor KN-93. Despite comparable degrees of SR Ca loading ($\int I_{Na/Ca}$=103.8±9%, caffeine contraction=103±6%) and peak I_{Ca} (103.5±3%), the contraction elicited for a given I_{Ca} was much smaller in KN93 (38.6±4%, n=7, p<0.0001). This resulted in a downward shift of the I_{Ca}-contraction relationship for a given SR Ca load. The effect of KN93 could be reversed and was not mimicked by the inactive analog KN-92. We conclude that CaMKII increases the responsiveness of Ca-induced Ca-release during cardiac E-C coupling.

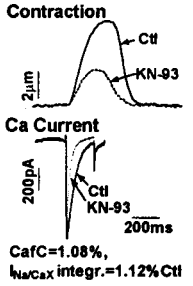

W-AM-I5

TIME COURSE OF CALCIUM INFLUX DURING THE CARDIAC ACTION POTENTIAL IN ISOLATED GUINEA PIG VENTRICULAR MYOCYTES. ((C.J. Grantham and M.B. Cannell)), Dept. of Pharmacology, St. George's Hospital Medical School, London SW17 0RE.

Action potentials (APs) were recorded from enzymatically isolated guinea-pig ventricular myocytes and used as the command waveform for conventional whole cell patch clamp measurements (Doerr et al., 1990). The AP recorded in physiological saline at 37°C rose from a resting potential of -84mV to a peak potential of +47mV and had a duration of 200ms. When cells were voltage clamped with this waveform at 37°C, using a K^+-based patch electrode filling solution in the presence or absence of 10mM BAPTA the ICa had a multiphasic time course which contrasted with the biphasic ICa evoked by a conventional voltage step. Analysis of these data suggest that 1) reverse INaCa contributes <30% of the Ca^{2+} influx which triggers SR release and 2) that more Ca^{2+} enters towards the end of the AP than would be anticipated. We suggest that the latter may be a feedback mechanism designed to limit variations in contractility due to variability in SR calcium loading. This view is supported by experiments which show that there is a large increase in Ca^{2+} influx if SR Ca^{2+} release is reduced.

Doerr, T., Denger, R., Doerr, A. and Trautwein, W. (1990) *Pflügers Arch.* 416, 230-237

Supported by the British Heart Foundation

W-AM-I6

SARCOPLASMIC RETICULUM CALCIUM CONTENT OF RAT CARDIAC MYOCYTES IN CALCIUM OVERLOAD. ((M.E. Díaz, A.W. Trafford, S.C. O'Neill & D.A. Eisner)) Veterinary Preclinical Sciences, The University of Liverpool, PO Box 147, Liverpool, L69 3BX, U.K.

Spontaneous oscillations of intracellular calcium concentration ($[Ca^{2+}]_i$) in cardiac myocytes are generally accepted to indicate overload of the sarcoplasmic reticulum (s.r.) with calcium .The present experiments were designed to investigate the possibility that spontaneous release occurs when the s.r. Ca content has reached a critical level. We have measured the s.r. Ca content under different degrees of cellular Ca loading by integrating the Na/Ca exchanger current following release of Ca from the s.r. by caffeine under voltage clamp conditions. We varied the degree of cellular Ca load by changing the external Ca concentration. In quiescent cells bathed in 1 mM external Ca, the s.r. content is 92.9 ± 12.8 (n = 8 ± s.e.m.). Under the same conditions the average s.r. content in oscillating cells, as expected, is higher; (120.8 ± 12.0 (n = 12)). However the cells oscillating in 1 mM Ca showed an increase, not only in oscillation frequency, but also, in the s.r. content when extracellular Ca was raised to 2 mM. These results suggest that spontaneous oscillations of $[Ca^{2+}]_i$ do not indicate that the s.r. has reached its maximum capacity. Oscillations frequently are initiated from the same site in the cell, and it is therefore possible that only this region of s.r. is overloaded. The increase of observed s.r. Ca content would then be ocurring in the rest of the cell.

W-AM-I7

ESTIMATION OF NET CALCIUM FLUXES IN FERRET VENTRICULAR MYOCYTES FOLLOWING SARCOPLASMIC RETICULUM CALCIUM DEPLETION BY CAFFEINE. A.W.Trafford, M.E. Díaz, †N.Negretti, S.C. O'Neill, D.A. Eisner. Veterinary Preclinical Science, University of Liverpool, U.K. and †Universidad Central de Venezuela, Venezuela.

An important factor determining the magnitude of the systolic Ca transient in cardiac ventricular myocytes is the amount of Ca released from the sarcoplasmic reticulum (SR). The Ca content of the SR is in turn regulated by the net movements of Ca across the surface membrane and the sarcoplasmic reticulum in response to changes in the stimulation protocol. In the present experiments the Ca content of the SR was estimated from the net movements of Ca across the surface membrane following depletion of the SR by caffeine and compared with the measured content obtained by subsequent caffeine applications. The integrals of the Ca current (I_{Ca}) and the Na-Ca exchange current ($I_{Na\text{-}Ca}$) were measured using the whole cell voltage clamp technique. Refilling of the SR following caffeine application was associated with a negative I_{Ca} and positive $I_{Na\text{-}Ca}$ staircase. The early transients following caffeine removal were associated with a net Ca gain by the cell, as the steady state I_{Ca} and $I_{Na\text{-}Ca}$ were reached this was associated with the influx and efflux pathways balancing and no net movement of Ca across the sarcolemma.

The pattern of amplitude of the intracellular Ca transient also exhibited a positive staircase and was correlated to the predicted SR Ca content. The present results indicate that the SR Ca content can be predicted from the net movements of Ca across the sarcolemma on the calcium and Na-Ca exchanger

W-AM-I8

LOW CONCENTRATIONS OF Cd^{2+} BLOCK I_{Ca} BUT NOT CONTRACTION IN CAT VENTRICULAR MYOCYTES. ((J. Andrew Wasserstrom and Ana-Maria Vites)) Department of Medicine, Northwestern University Medical School, Chicago, IL, 60611.

We investigated the effects of low concentrations of Cd^{2+} on I_{Ca} and cell shortening in isolated cat ventricular myocytes using whole the cell voltage clamp technique at 34°C. Holding potential was -40mV and test potentials ranged from -30 to +100mV. Each test voltage step was preceded by 2-3 conditioning steps to +100mV (100-500msec) in order to insure replenishment of SR Ca^{2+} stores before each test pulse. A concentration of 20μM Cd^{2+} blocked I_{Ca} by 97±1.5% (n=5). In contrast, cell shortening (in K^+-containing solutions) was reduced to 62±23% of control (n=8) during superfusion with 20μM Cd^{2+}. Block was nearly equivalent at all test potentials, suggesting a lack of voltage dependence. Addition of ryanodine blocked all contractions, indicating that cell shortening was the result of Ca^{2+} release from the SR (n=3). Exposure to Ni^{2+} (4mM, n=4) also blocked Cd^{2+}-insensitive contractions, suggesting that reverse mode Na-Ca exchange might be involved in activation of cell shortening in the absence of I_{Ca}. These results suggest that 1) activation of contraction occurs despite block of I_{Ca} by a low concentration of Cd^{2+}; 2) activation does not require Ca^{2+} influx via I_{Ca} but does require that the SR contain adequate Ca^{2+} stores such as occur under physiological conditions; and 3) activation of Cd^{2+}-insensitive contractions may occur secondary to Ca^{2+} influx via reverse mode Na-Ca exchange which triggers release of Ca^{2+} from the SR that is rapid enough and of sufficient magnitude to cause E-C coupling in heart.

W-AM-J1

SINGLE MOLECULE DETECTION BY TWO-PHOTON EXCITED FLUORESCENCE ((Jerome Mertz, Chris Xu, and Watt W. Webb)) Dept. of Applied Physics, Cornell University, Ithaca, NY 14853.

We demonstrate a technique for localizing and detecting individual fluorescent molecules in solution based on two-photon excitation (TPE). A mode-locked laser beam is focused into the solution, thereby defining a TPE volume localized in three dimensions. Molecules diffusing in and out of this volume produce fluorescence bursts which are detected with a high signal-to-background ratio. The theoretical foundations for this technique are derived, including an analysis of the sampling dynamics and attendant fluorescence rate probability distributions. These agree with experimental results obtained for single rhodamine-B molecules in water.

Funded by NSF (BIR8800278) and NIH (RR04224 and RR07719) at the Developmental Resource for Biophysical Imaging and Opto-Electronics.

W-AM-J2

DEPENDENCE OF SPIN-LABEL SATURATION TRANSFER EPR INTENSITIES ON SPIN-LATTICE RELAXATION. ((T. Páli and D. Marsh)) Max-Planck-Institut für biophysikalische Chemie, Abteilung Spektroskopie, Am Faßberg, D-37077 Göttingen, Germany.

The intensities of saturation transfer (ST) EPR spectra from nitroxyl spin labels have proved a sensitive means for studying slow exchange processes (both Heisenberg spin exchange and physical/chemical exchange) and interactions with paramagnetic ions, via the dependence on the effective spin-lattice relaxation rate (e.g. Marsh, *Applied Mag. Reson. 3*, 53, 1992). The dependences of the second harmonic EPR absorption intensities detected in phase quadrature with the field modulation (V_2'-display) on the microwave H_1-field, and on the effective relaxation times, were studied both theoretically and experimentally. Power saturation curves and normalized integrated intensities (I_{ST}) of the V_2'-spectra were determined as a function of concentration of a spin-labelled phospholipid in lipid membranes, as a means of varying the effective relaxation times. The results were correlated with progressive saturation measurements of the double-integrated intensities of the conventional EPR spectra. Intensities of the V_2'-spectra were calculated from the Bloch equations incorporating the modulation field (Halbach, *Helv. Phys. Acta 27*, 259, 1954) and the results fitted to the experimental data. The ST-EPR intensities, I_{ST}, depend approximately linearly on the effective T_1-relaxation time, but with a non-zero intercept. On the basis of the theoretical calculations, alternative calibrations are suggested between I_{ST} and T_1 that may improve precision in the application of this alternative form of ST-EPR spectroscopy to biological systems. The present results refer to the diffusional collisions of lipids in membranes.

W-AM-J3

Quantitative Measurement of Electrorotation and its Dependence on the Surface Charge

((H. Maier)) ENT Hearing Research Laboratories, University of Tuebingen, 72076 Tuebingen, Silcherstr. 5, Germany.

An electrorotation apparatus with an three electrode configuration for the frequency range between 50Hz and 20 Mhz will be presented. With this device, rotating and gradient fields of defined precision and homogeneity can be applied to slightly conducting suspensions. The numerical calculation of the electric field distribution in combination with defined boundary conditions allows the determination of the resulting torque applied on the suspended spheres. Latex particles were characterized in their chemical composition and separated according to their electrophoretic mobility to improve accuracy in measured rotation velocity. Electrorotation spectra of suspensions of different ionic strength and surface charge were recorded. In addition the dependence of the rotation at the Maxwell-Wagner-Frequency (M-W-F: $\omega_o = \sigma_l / \varepsilon_l \varepsilon_o$ l: liquid) on the ionic strength and the surface charge were examined in detail. The behavior for vanishing surface charges could be demonstrated for the first time. For the dependence of rotation at the M-W-F on the surface charge a model was developed and solved numerically describing the dependence on the surface charge. The results show that the description of dielectrophoretic and electrorotation phenomena has to include surface charges with the associated hydrodynamic problem in an adequat manner. Current hypothesises and theories have to be reconsidered with this data in mind.

W-AM-J4

A MODEL OF HYDRATION OF INVERTED HEXAGONAL (H_{II}) PHASE OF PE.,(M. Ge, and J.H. Freed)), Baker Lab of Chemistry, Cornell University, Ithaca, NY 14853

Since phosphatidylethanolamins (PEs) in the H_{II} phase are more hydrated than in the L_α phase, we suggest that in the H_{II} phase, part or all of the hydrogen bonds between the PE headgroups in the direction of the tube axis break. Thus, the walls of the tubes are wetted and the hydration of the H_{II} phase can be interpreted as a process of condensation of water in capillaries. That is, upon hydration the change in the structural dimensions is driven by the surface tension effects on two interfaces: the water-vapor interphase (meniscus) at the ends of the tube and the lipid-water interphase inside the tube. It turns out that at a low level of hydration, there is a large tension (negative pressure) along the axis of the water column. Upon increasing the water vapor pressure, this tension decreases exponentially as the radius of the water core (r) increases. The hydration process would continue up to the point of the zero osmotic pressure, where all the menisci are flat and the tension vanishes. Further increase in the water content will result in the coexistence of the H_{II} phase and excess water. On the other hand, there is a large compression (positive pressure) perpendicular to the axis of the water column at low hydration, which varies with r^{-1}, i.e., it also decreases as the water content increases. However, at limiting hydration, this pressure does not vanish and still remains greater than the surrounding pressure.

W-AM-J5

FLUORESCENCE DECAY OF DODCI AND OTHER DYES IN EGGPC MEMBRANE: EFFECT OF EXTERNAL VISCOSITY AND REFRACTIVE INDEX. ((M.M.G. Krishna and N. Periasamy)) Chem. Phys. Gp., T.I.F.R., Bombay-400005, India (Spon. by S. Tripathi)

Fluorescence decay of DODCI in EggPC vescicle membrane is biexponential with lifetimes, 1.76 ns(0.37) and 0.73 ns(0.67), at 25C. The emission spectra associated with the lifetimes show peaks at 615 nm (1.76 ns) and 595 nm (0.73 ns). The steady state and decay associated spectra indicate the presence of two spectroscopically distinct species of DODCI. The presence of sucrose (upto 44.4% w/w) in the aqueous phase decreases the lifetime of 1.76 ns component (effect of increasing refractive index), and increases the lifetime of 0.73 ns component (effect of increasing viscosity). The localization of the two species in the membrane is different: one species is buried in the membrane and the other exposed to the aqueous phase. The influence of external refractive index and viscosity on the lifetimes is absent or less pronounced for nile red, rhodamine 6G, and $diIC_{18}(3)$.

W-AM-J6

BIOPHYSICAL CHARACTERIZATION OF BIS-MALEIMIDE PEG2000 INTRAMOLECULARLY CROSSBRIDGED HEMOGLOBIN.

((D.S.Gottfried, E.S. Peterson, S, Huang, J. Wang, R.E. Hirsch, S. Acharya, and J.M. Friedman.)) Department of Physiology and Biophysics, Albert Einstein College of Medicine, Bronx, NY 10461

HbA intramolecularly crossbridged with bis-Mal PEG2000 retains both cooperativity and near normal oxygen affinity despite the fact that the site of attachment is Cys β93. Most simple modifications of this site produce high affinity Hbs with drastically reduced or eliminated cooperativity. The purpose of the present study is to determine how the reaction of bis-maleimide PEG 2000 modifies the overall tertiary and quaternary conformations of HbA and thus alters ligand rebinding kinetics. Upon switching from the deoxy to the carbonmonoxy derivative of the bis-Mal PEG crossbridged HbA, the α1β2 interface undergoes transitions that are very similar to those that occur when HbA undergoes the T to R quaternary switch; however ultraviolet RR results indicate that the presence of this crossbridge enhances the hydrogen bonding between the penultimate tyrosines and its hydrogen bonding partner on the FG corner. An increase in this interaction is expected to impart "T" like properties to the R state of the liganded form of the protein. The decreased iron-proximal histidine stretching frequency in the 10 ns visible Raman spectrum supports this interpretation. Flash photolysis studies reveal a reduction in the amount of geminate recombination in this derivative compared to HbA and several other crossbridged Hb's. Titration curves for HPT, using time-correlated single photon counting fluorescence lifetime measurements, demonstrate that HPT binds more extensively to bis-Mal PEG crossbridged COHbA than to COHbA (which shows greater binding than a β82 crossbridged derivative). The increased HPT binding is consistent with enhanced proximal strain for the CO bound bis-Mal PEG derivative compared to COHbA.

W-AM-K1

PROTEIN BINDING TO LIPID MEMBRANES AND ITS INFLUENCE ON HEAT CAPACITY PROFILES AND PROTEIN AGGREGATION. ((T. Heimburg*+, D.Marsh+, and R.L.Biltonen‡)) +Max-Planck-Institute for Biophysical Chemistry, 37077 Göttingen, Germany, and ‡Dept. of Biochemistry, University of Virginia, Charlottesville, VA 22908

The interaction of peripheral proteins with charged lipid membranes has been investigated using the analysis of binding isotherms (Heimburg and Marsh, 1995), calorimetry and statistical thermodynamics calculations. The binding was shown to induce shifts of the heat capacity profiles and aggregation of proteins in the lipid melting regime is predicted.
From the analysis of the binding of cytochrome c to charged lipid membranes, the effective charge of the protein, the lipid/protein stoichiometry and the intrinsic binding constants were obtained. The difference of the protein binding free energy to the lipid fluid phase with respect to the lipid gel phase was calculated. This difference gives rise to a shift in the heat capacity maximum, that is consistent with the shift found in calorimetric measurements. To explain the heat capacity profiles we described the interaction of proteins with lipids on the basis of an Ising-model that uses an interfacial free energy contribution of adjacent lipid molecules to rationalize the cooperativity of the lipid melting transition. An additional free energy contribution originates from the interaction of proteins with lipids and was obtained from the binding analysis. We simulated the dynamics and the heat capacity profiles of the lipid-protein system using a Monte Carlo computer simulation. Shifts of the heat capacity maxima caused by protein binding suggest a preferential binding of the protein to the lipid gel state in the cytochrome c -DMPG model system. This leads to aggregation of proteins on the lipid surface in the range of gel/fluid coexistence. The lipid melting curves are shifted and broadened as a consequence of protein binding. All parameters used can be obtained directly from experiments.

W-AM-K2

STOPPED-FLOW FLUOROMETRIC STUDY OF THE INTERACTION OF MELITTIN WITH PHOSPHOLIPID BILAYERS: IMPORTANCE OF THE PHYSICAL STATE OF THE BILAYER AND THE ACYL CHAIN LENGTH. ((Thomas D. Bradrick, Alexander Philippetis and Solon Georghiou)) Molecular Biophysics Laboratory, Physics Department, University of Tennessee, Knoxville, TN 37996.

Stopped-flow fluorometry has been employed to study the effects of melittin, the major protein component of bee venom, on dimyristoylphosphatidylcholine (DMPC) and dipalmitoylphosphatidylcholine (DPPC) small unilamellar vesicles (SUVs) on the millisecond time scale, before melittin-induced vesicle fusion takes place. Use is made of 1-(4-trimethylammoniumphenyl)-6-phenyl-1,3,5-hexatriene (TMA-DPH), which is an oriented fluorescent probe that anchors itself to the bilayer-water interface and is aligned parallel to the normal to the bilayer surface; its fluorescence anisotropy reports on the "fluidity" of the bilayer. For DMPC bilayers, melittin is found to decrease their fluidity only at their melting transition temperature. This perturbation appears to be exerted almost instantaneously on the millisecond time scale of the measurements, as deduced from the fact that its rate is comparable to that obtained by following the change in the fluorescence of the single tryptophan residue of melittin upon inserting itself into the bilayer. The perturbation is felt in the bilayer over a distance of at least 50 Å, with measurements of transfer of electronic energy indicating that the protein is not sequestered in the neighborhood of TMA-DPH. The length of the acyl chains is found to be an important physical parameter in the melittin-membrane interaction: unlike the case of DMPC SUVs, melittin does not alter the fluidity of DPPC SUVs and has a considerably greater affinity for them. These results will be discussed in terms of the concept of elastic distortion of the lipids, which results from a mismatch between the protein and the acyl chains that are attempting to accommodate it. Melittin is also found to cause a small (~10%) enhancement in the total fluorescence intensity of TMA-DPH, which we interpret as indicating a reduction in the degree of hydration of the bilayer. (This work was supported in part by National Institutes of Health research grant GM32433.)

W-AM-K3

Structure and Interaction of A Transmembrane Polyalanine α-Helix with a DMPC Bilayer Studied by Multi-nanosecond Molecular Dynamics Simulation ((Liyang Shen, Donna Bassolino, and Terry Stouch)) Bristol-Myers Squibb, P.O.Box 4000, Princeton, NJ 08543-4000.

We have performed all-atom multi-nanosecond molecular dynamics simulations to study $(Ala)_{32}$-peptide-DMPC lipid bilayer system to understand the protein-membrane structures and interactions. The polyalanine was built initially of a α-helical structure. The helical stability of the peptide varied, dependent on its location in the bilayer. The middle segment residing in the hydrocarbon chain region, maintained a very stable α-helix, while the two terminal segments, located in the lipid headgroup region and the water/lipid interface, unfolded and experienced a number of different coiled structures over the 1.66 ns simulation time. The helical segment tilted dynamically from the bilayer normal with a mean angle of 32°. The rotational time correlation function calculations revealed that the half of the helical segment rotated with $\sim 90°$ over 1.66 ns, however the other half had essentially no rotation. Lateral translation of the peptide was larger than transverse; the calculated lateral diffusion constant was $7.9 \times 10^{-7} cm^2/s$. Electrostatic interactions and H-bonding between the terminal residues and lipid headgroups/water molecules were observed. The longest H-bond residence time was 0.68 ns. Lipid population distribution around the peptide were analyzed in great detail. Statistically, there were 18 lipid molecules with atoms within 5.0 $\AA$ close to the peptide. A wide variety of lipid conformations was observed. The mean tilting of the P-N vectors was 89° from the bilayer normal with a standard deviation of 69° and that of the hydrocarbon chains $\sim 35°$ with the standard deviation of $\sim 57°$. Bulk properties of the bilayer with and without the peptide did not change significantly.

W-AM-K4

Scanning Probe Microscopy Study of MonoGalactosylDiacylGlycerol / Cytochrome *f* Langmuir-Blodgett Films.
A. Tazi, S.Boussaad, and R.M. Leblanc, Department of Chemistry, P.O. Box 249118, University of Miami, Coral Gables, Florida 33124-0431 USA

The dominant lipids of thylakoids membranes are uncharged galactolipids, monogalactosyldiacylglycerol (MGDG) and digalactosyldiacylglycerol (DGDG). It has been suggested that specific lipids, especially MGDG, may be found at the lipid/protein interfaces, fitting around the lipid/protein complexes[1]. In this study, the goal was to observe a change in the protein behavior, if any, when the protein is mixed with a lipid. We report in this study the topography of a mixed single layer of MGDG/Cyt *f*, imaged with the scanning probe microscopes (SPM), i.e. the scanning tunneling microscope (STM) and the atomic force microscope (AFM). The monolayer was transferred at 26 mN/m onto freshly cleaved mica and Au(111). We have noticed that Cyt *f* tends to form aggregates[2] (average size ~ 50 nm) and in the presence of the lipid (MGDG), the aggregates appear as a cone shape. We have obtained high resolution images of the aggregated cones of Cyt *f* where the shape of a single protein (average size ~ 5 nm) can be recognized. The molecular area calculated from SPM images (~ 20 nm²) is in agreement with the estimated area from the Π-A isotherms[3].

[1]: D.J. Murphy, Biochim. Biophys. Acta, 864, 1986, 33-94.
[2]: A. Tazi, S. Boussaad and R.M. Leblanc, *Submitted to Biochimica Biophysica Acta*
[3]: A. Tazi, S. Hotchandani, G.Munger and R.M. Leblanc. Thin Solid Films, 247, 1994, 240-243.

W-AM-K5

TRANSBILAYER TRAFFIC OF IONS AND LIPIDS COUPLED TO MASTOPARAN X TRANSLOCATION ((K. Matsuzaki, S. Yoneyama, and K. Miyajima)) *Faculty of Pharmaceutical Sciences, Kyoto University, Sakyo-ku, Kyoto 606-01, Japan*

Recently an amphiphilic peptide, magainin 2 has been shown to translocate across lipid bilayers by forming a pentameric pore. [1,2] and to simultaneously induce the rapid flip–flop of membrane lipids [3]. In this paper, we will demonstrate that a wasp venom, mastoparan X also induces coupled transbilayer movement of the peptide, ions, and lipids. The peptide translocation was proved by three different experiments mainly using resonance energy transfer from tryptophan of the peptide to a dansylated lipid incorporated into the lipid vesicles. The translocation was coupled to the pore formation, as detected by the efflux of a fluorescent dye, calcein, from the liposomes. The lipid flip–flop was measured based on the reduction of a NBD-labeled lipid by a water soluble reagent, sodium dithionite. Our results suggest that the translocation of the peptide quantitatively generates two signals, i.e., an ion pulse and a lipid pulse which shortcircuit the otherwise insulated two aqueous phases and lipid monolayers, respectively.
[1] Matsuzaki, K., et al., *Biochemistry* **34**, 6521 (1995).
[2] Matsuzaki, K., et al., *Biochemistry* **34**, in press (1995).
[3] Matsuzaki, K., et al., The 23rd FEBS Meeting, Basel (1995).

W-AM-K6

COLIPASE INTERACTIONS WITH LIPIDS ((H.L. Brockman, M. Momsen and W. Momsen)) Hormel Institute, U of MN, Austin, MN 55912.

Pancreatic lipase uses a protein cofactor, colipase, to provide an adsorption site at the lipid-water interface. We recently reported that the pro form of colipase interacts preferentially with lipase substrates as compared with matrix phospholipids. In the present study adsorption of ^{14}C-colipase to monolayers of 1-stearoyl-2-oleoyl phosphatidylcholine [SOPC] and either 13,16-*cis,cis*-docosadienoic [DA] acid or 1,3-dioleoylglycerol [DO] was measured as a function of lipid concentration and composition. With SOPC monolayers, ^{14}C-colipase adsorption increased the surface pressure to ~ 27 mN/m at all initial surface pressures below this value. With DA or DO maximal surface pressures were as high as 42 mN/m and 34 mN/m, respectively, values which exceed by 4-6 mN/m the collapse pressures of the lipids alone. These data show that the interaction of colipase with DA or DO is stronger than that observed earlier with procolipase, supporting the notion of a functional role for the proteolytic activation of procolipase. The quantity of colipase adsorbed to mixed-lipid monolayers approximately obeyed the simple geometric model reported earlier. However, the data obtained using ^{14}C-colipase with the improved assay suggests a model in which lipid molecules preferentially fill voids between colipase molecules, then forms an annulus around them and finally separate the colipase molecules further(SOPC) or are expelled from the surface(DO or DA). Supported by HL 49180 and the Hormel Foundation

W-AM-K7

ENZYMIC FORMATION OF CYCLIC LYSOPHOSPHATIDIC ACID MONITORED BY ^{31}P NMR.

Peter Friedman[1], Ofer Markman[2], Rachel Haimovitz[1],
Mary F. Roberts[2] and Meir Shinitzky[1]
The [1]Department of Membrane Research and Biophysics, Weizmann Institute of Science, Rehovot, ISRAEL and the [2]Department of Chemistry, Boston College, Chestnut Hill, Boston, MA, USA.

^{31}P-NMR provides a powerful tool for monitoring kinetics of enzymic reactions, in particular phospholipases, while they take place in the NMR tube. In such an experimental setting we have discovered a novel phospholipid, cyclic lyso phosphatidic acid, which appears as an intermediate in the cleavage of lyso phospholipids by PLaseD. Upon the formation of the enzyme-substrate complex intramolecular trans phosphorylation takes place through the free ß-hydroxyl group of the glycerol backbone which acts as a nucleophile. This cyclic phosphate is further hydrolysed to lyso phosphatidic acid. An attempt to slow down the latter process by introduction the phosphate analog - vanadate, yielded a pyro phosphovanadate complex which is stabilized by coordinative bonds of Ca^{2+}, an assignment which was supported by ^{51}V NMR. Our findings on the PLaseD (from *Streptomyces Chromofuscus*) indicates that this enzyme is of dual activity: phospholipase and phosphodiesterase.

Analogous findings were observed while introducing lysophospholipids into human plasma. The formation of the cyclic intermediate, cyclic-LPA, was observed again. This activity is assumed to be enzymic, since inactivated serum was void of such activity.

W-AM-K8

NON ADHESIVE PROPERTIES OF POLYSACCHARIDES.

(E.Romero, S. Porro, and S. Alonso - Romanowski). Departamento de Ciencia y Tecnología. Universidad Nacional de Quilmes. R Sáenz Peña 180. (1876) Bernal. ARGENTINA.

Neural cell adhesion molecules (NCAMs) can undergo post-translational modifications, such as the addition of polysialic acid chains, thus generating PSA-NCAMs, which are expressed mainly during developement. Since polysialylation considerably modifies NCAM adhesivity, we decided to investigate if the multilamellar liposomes prepared in the presence of polysialic (PSA) and sialic acid (SA) have adhesive properties when reacting with human plasmatic proteins.

First we determined the incorporation of SA and PSA to MLV using merocyanine 540 as a probe and the degree of incorporation of the sugars by reverse phase HPLC. To determine whether PSA-MLV bind plasmatic proteins, the multilamellar vesicles (MLV) containing PSA were incubated with human plasma. The PSA-MLVs, subsequently analysed by SDS-PAGE showed non adhesive properties, which will permit longer lived stabilized liposomes in blood stream.-

W-AM-K9

INTERACTION OF PULMONARY SURFACTANT PROTEINS SP-B AND SP-C WITH BILAYERS OF DPPC, STUDIED BY FLUORESCENCE SPECTROCOPY

((Jesús PEREZ-GIL, Antonio CRUZ, Ines PLASENCIA and Cristina CASALS))
Dept. Bioquímica y Biología Molecular I, Fac. Biología. Univ. Complutense. 28040 Madrid (SPAIN).

Porcine SP-B and SP-C have been reconstituted in DPPC vesicles by mixturing small volumes of solutions of DPPC in methanol and protein in acetonitrile/water 70%, and injecting the mixture in buffer HEPES 50 mM, NaCl 150 mM, pH 7. Interaction of SP-B with DPPC produced a significant increase in the intensity of the fluorescence emission spectrum of the protein, with excitation at 275 nm, accompanied by a blue-shift of the wavelength of the emission peaks of the spectrum from 330.5 and 342.5 to 325 and 337.5 nm, respectively. Reconstitution of SP-B at different SP-B/DPPC ratios allowed estimation of the apparent parameters of SP-B/DPPC interaction. The estimated apparent SP-B/DPPC dissociation constant, K_p, was 4.5 ± 1 10^{-6} M^{-1} and n, the lipid/protein stoichiometry, was 15 ± 2. The use of phospholipid spin probes as quenching agents, according to the parallax method, allowed to estimate that the distance of the tryptophan residue of the reconstituted SP-B to the center of DPPC bilayer was 9.8 ± 0.2 nm which is consistent with a superficial location of SP-B in the membrane.

On the other hand, the study of the interaction of porcine SP-C with DPPC vesicles was approached by covalently attaching a dansyle group to the N-terminal amine of the protein. Insertion of dans-SP-C in DPPC vesicles produced a shift in the wavelength of emission of the SP-C-attached dansyle fluorescence spectrum, from 487 to 507 nm using a excitation wavelength of 330 nm. This shift is interpreted as originated in the change of the environment of the probe from the aqueous bulk phase to the membrane surface. Reconstitution of dans-SP-C at different protein/DPPC ratios allowed to estimate an apparent K_0 of 5.2 ± 0.8 10^{-6} M^{-1} with $n = 4 \pm 1$. The espectroscopical properties of the dansyle group attached to SP-C reconstituted in DPPC bilayers suggest that the modified N-terminal end of the protein is not inserted in the bilayer, but exposed to the aqueous environment.

W-AM-K10

THE DETERMINATION OF HELIX ORIENTATION IN LIPID MEMBRANES BY POLARIZED ATIR-FTIR

((Mario J. Citra and Paul H. Axelsen))
Department of Pharmacology, University of Pennsylvania, Philadelphia PA

Polarized attenutated total internal reflection Fourier-transform infrared (PATIR-FTIR) spectroscopy may be used to characterize the orientational order of polypeptide helices. This technique requires knowledge of the applicable electric field amplitudes, and θ - the orientation of the vibrational transition moment relative to the helix axis. To examine these values, we have studied β-benzyl derivatives of poly-aspartate and poly-glutamate on the surface of an internal reflection crystal under conditions of known conformation and orientation. Our results indicate that (1) the aspartyl and glutamyl peptides manifest differing values for θ, despite similar amide I absorption frequencies and bandshapes; and (2) the absorption intensities for these polymers in a lipid membrane are self-consistent only if we assume the electric field amplitudes to be determined entirely by the refractive index of the bulk medium in which the crystal is immersed. These results suggest that three-phase (crystal-membrane-air/water) equations commonly applied in the analysis of PATIR-FTIR spectra may be misleading. When the bulk phase is water (n=1.32), the index typically used for lipid membranes (n=1.40) is not drastically different, and the error is probably small. When the bulk phase is air (n=1.00) however, the error can be substantial.

Supported by the L. P. Markey Charitable Trust and HL-47469

COMPUTER SIMULATIONS

W-AM-L1

NEAREST-NEIGHBOR WEDGE MODEL PARAMETERS OF CURVED DNA: ON THE EXISTENCE OF A UNIQUE SOLUTION AND ITS DERIVATION.

((A. Bolshoy and P. Furrer)) Dept. of Membranes Research and Biophysics, Weizmann Institute of Science, Rehovot 76100, Israel and Laboratoire d'Analyse Ultrastructurale, Université de Lausanne, Lausanne-Dorigny, Switzerland, CH-1015. (Spon. by J. Sussman)

In recent years much work has focused on curved DNA. The studies have demonstrated undoubtedly that certain double-stranded DNA molecules in the B-form have no straight axis in their relaxed state. It is of a practical importance to predict a sequence-dependent net-averaged DNA path for any given sequence. This could be achieved only on the basis of usage an appropriate model and statistical processing of experimental data to obtain parameters of the model. A nearest-neighbor wedge model of DNA structure was proposed earlier. The question can be asked: Is it possible in principle to derive a unique solution from statistical processing of experimental data on the basis of the model ? We tried to answer these questions by computer simulations, gedanken experiments. These experiments gave strong evidence that all parameters of the nearest-neighbor wedge model can be estimated with high accuracy by minimizing an average misfit between simulated "experimental" values and those calculated according to the model. The solutions generated (the sets of wedge angles) are unique in most of the simulated cases.

W-AM-L2

A FIRST-PASSAGE ALGORITHM FOR THE HYDRODYNAMIC FRICTION AND DIFFUSION-LIMITED REACTION RATE OF MACROMOLECULES.

((James A. Given, Joseph B. Hubbard, and Jack F. Douglas)), Center for Advanced Research in Biotechnology, Rockville MD 20850 and National Institute of Standards and Technology, Gaithersburg MD 20899

Many important properties of a macromolecule can be expressed in terms of averages over the trajectories of diffusing particles that begin in the medium surrounding the molecule and terminate at its surface. These properties include its translational hydrodynamic friction coefficient and the Smoluchowski rate constant for diffusion-limited reactions. In this paper we introduce a first-passage algorithm (FPA) for calculating such quantities efficiently and accurately. This algorithm uses certain exact Green's functions, or propagators, for the Laplace equation to eliminate the need to construct explicitly those portions of a diffusing particles' trajectory that are not near an absorbing object. The algorithm is especially efficient for studying objects that contain large voids or have very irregular surfaces. Diffusion algorithms were previously shown to give accurate results for the quantities we study. In this paper, we show that first-passage methods make these algorithms accurate and efficient. In future work, we expect to present systematic results for the properties of globular proteins.

W-AM-L3

RADICAL-PAIR RECOMBINATION KINETICS IN ENZYMATIC REACTIONS UNDER MAGNETIC FIELD INFLUENCE: A THEORETICAL STUDY. ((C.F. Eichwald and J. Walleczek)) Stanford University School of Medicine, Stanford, CA 94305. (Spon. by A. Saad)

Recent experimental studies have shown magnetic field effects on the enzymatic reaction of B_{12} ethanolamine ammonia lyase (Harkins & Grissom, Science 263 (1994) 958). Magnetic fields in the milli-Tesla range exert an influence on the recombination kinetics of a transient pair of free radicals that is formed during the enzyme reaction cycle (radical-pair-mechanism). We present a theoretical model that describes magnetic field effects in enzymatic reactions. The model is an extended Michaelis-Menten scheme. The extension consists in the inclusion of a secondary enzyme-substrate complex where a transient free radical pair exists. This enables calculation of the reaction rate as a function of the rate constant for the radical pair recombination step. The magnetic field influence on this particular rate constant is calculated using the "exponential model" for radical pair recombination, which is a simple quantum-statistical approach for radical pair recombination steps known from magnetochemistry. Model simulations qualitatively reproduce the experimentally observed changes in enzyme activity in dependence on magnetic flux density (reduction in V_{max}/K_M for low flux densities and increases for high flux densities). The model predicts that the size of the magnetic field effect on the catalytic activity of the enzyme depends critically on the relation between the time-scales inherent to the chemical rate constants and those induced by the different magnetic interactions (singlet-triplet conversion ratio due to hyperfine interactions and difference in g-value of radicals).

W-AM-L4

DETERMINATION OF PROTEIN INFLUENCES ON THE STRUCTURE AND DYNAMICS OF THE HEME IN MYOGLOBIN. ((T. Rush III and T.G. Spiro)) Department of Chemistry, Princeton University, Princeton, NJ 08544.

With the aid of normal mode calculations in Cartesian coordinate space and molecular mechanics calculations, the influence of the apoprotein on the structure and dynamics of the heme in myoglobin is being studied. To accurately model the structure and dynamics, our consistent empirical valence force field for protoporphyrins and Scheraga *et al*'s quantum mechanically derived protein atomic charges [1] were combined to form the major part of the force field for this work. A discussion of the predicted geometries and heme vibrational frequencies will be presented along with a comparison between the results obtained with our and other biomolecular force fields.

1. Chipot, C., Maigret, B., Rivail, J-L. and Scheraga, H.A. (1992) *J. Phys. Chem.*, 96, 10276-10284; *ibid*, (1993) 97, 9788-9796; *ibid*, (1993) 97, 9797-9807.

W-AM-L5

PROTEIN SUBSTATE MODELING AND IDENTIFICATION USING THE SINGULAR VALUE DECOMPOSITION. ((T.D. Romo, J.B. Clarage, †D.C. Sorensen, G.N. Phillips, Jr.)) Department of Biochemistry and Cell Biology, †Department of Computational and Applied Mathematics, Rice University, Houston, TX 77005-1892

Time-averaged and multi-conformer crystallographic refinements are two methodologies for modeling the different substates accessible to protein in a crystal. Multi-conformer refinements use multiple structures, each contributing equally to the structure factor calculation. These structures are separated by simulated annealing with differing seeds, and represent different regions of the phase space accesible to the protein. Time-averaged refinement is an extension of molecular dynamics where the average structure is restrained to fit the observed X-ray data. With this methodology, an ensemble of structures consistent with both the dynamics force-fields and the observed data is generated that represent a range of conformations accessible to the protein in the crystalline state. Here, a comparison is made between these refinement schemes for a synchrotron CO-Myoglobin dataset using data to 1.3 Å resolution.

The singular value decomposition or SVD is an important and popular matrix decomposition that can be used to analyze the ensemble of structures and visualize the phase space accessible to a protein. The SVD constructs a basis set of vectors that describe the modes of atomic motion in the dynamics trajectory. What sets the SVD apart for the more traditional eigendecomposition analysis is that it includes temporal information. Combining the spatial and temporal information, the SVD is able to locate substates for any unit of the protein, such as a residue that swings between two distinct conformations.

This work supported by NIH, NLM, NSF, The W.M. Keck Center for Computational Biology, and the Robert A. Welch Foundation.

W-AM-L6

ANALYTICAL METHOD FOR MOLECULAR SHAPES: AREA, VOLUME, CAVITIES, INTERFACE AND POCKETS
((Jie Liang[1,2], Herbert Edelsbrunner[2], Sudhakar Pamidghantam[3], Shankar Subramaniam[1,3])) [1]NCSA, Beckman Institute, and [2]Dept. of Computer Science, and [3]Dept. of Molecular and Integrative Physiology & Program in Biophysics and Computational Biology, University of Illinois at Urbana–Champaign,Urbana, IL 61801

Shapes are important in molecular recognition, molecular docking, protein thermodynamics, solvation, and folding. New insights into molecular shapes can be obtained by using alpha-shape method developed in computational geometry. This method takes advantage of the duality of weighted Voronoi decomposition and Delaunay triangulation. We describe the concepts and ideas underlying the alpha shape method, as well as the algorithmic design of a suite of tools for molecular modeling. We report our results in computing molecular metric properties (area and volume), inaccessible cavities of proteins, and describe an approach for analyzing protein-protein interfaces. The latter has implications for protein association and thermodynamics. Further, we have developed a novel alpha shape-based tool for computing shapes of binding pockets and active sites and the cast of the complement space in enzymes. We demonstrate the power of these methods through several applications. Supported by grants from the National Science Foundation.

W-AM-L7

NAVIGATING THE PROTEIN FOLDING ENERGY LANDSCAPE ((N.D. Socci and J.N. Onuchic)) Department of Physics, University of California at San Diego, La Jolla CA 92093-0319.

In the spirit of the physics of phase transitions, experimental information on the structure and dynamics of the molten globule supplemented by a simple theory of the helix coil transition in collapsed heteropolymers can be used to find the global characteristics of the energy landscape for the folding of highly helical proteins. These results allow us to establish a law of corresponding states relating simulations of simple lattice models to real proteins which possess many more degrees of freedom. We study in detail the folding dynamics of a simple three dimensional lattice model. A reasonable reaction coordinate for folding is determined and then various thermodynamics and kinetic quantities (such as the free energy, correlation times and diffusion coefficients) are measured using Monte Carlo simulations. We find that simple diffusive rate theory predicts extremely well the folding times of the full simulations. Folding in this system is best viewed as a diffusive, funnel-like process.

* Supported by the Arnold and Mabel Beckman Foundation, the University of California, San Diego Chancellor's Fellowship (to N.D.S) and the NSF (Grant# MCB9316186).

W-AM-L8

MOLECULAR DYNAMICS SIMULATIONS OF INDIVIDUAL BACTERIORHODOPSIN HELICES ((Thomas B. Woolf)) Depts of Physiol. and Biophys., Johns Hopkins Univ., Schl of Med, Baltimore, MD 21205

Molecular dynamics simulations of the seven helices of bacteriorhodopsin were performed in explicit DMPC lipid. The program CHARMM was used with either hexagonal periodic boundary conditions or with a new constant pressure algorithm (Feller, Pastor and Venable, in press). The results, from at least 250 psec for each helix, showed the existence of domains of motion dependent on the sequence. Helices whose ends contained aromatics tended to be strongly anchored. Those with both aromatics and charges were less constrained and those with neither were the most mobile. The proline residues in helices B, C, and F separated the motion into two distinct domains. This is shown with ten snapshots separated by 25 psec each for helix C in the figure. These results were further analyzed in terms of the local energetic interactions at the helical ends mediated by either charged or aromatic residues and by the effect of proline as a helix breaker. Interaction energies were also calculated between the helices and DMPC molecules. The results support the emerging idea that weak protein:lipid interactions are dominated by VDW contacts and stronger interactions involve nearly an equal contribution from electrostatic and VDW energies.

W-AM-L9

INTERACTIONS OF SMALL SOLUTES WITH MEMBRANES ((A. Pohorille, M. A. Wilson and C. Chipot)) Dept. of Pharmaceutical Chemistry, Univ. of California, San Francisco, CA 94143 and NASA-Ames Research Center, Moffett Field, CA 94035 (Spon. by L. R. Pratt)

The behavior of 15 small solutes at the water–membrane interface was investigated. The free energy of nonpolar molecules decreases monotonically from water to the membrane interior. In contrast, the free energy of solutes that exhibit some polarity has an interfacial minimum which arises from superposition of two monotonically and oppositely changing contributions: electrostatic and nonelectrostatic. Conformational preferences of flexible solutes depend on their position in the water–membrane system and, conversely, the structure and dynamics of the membrane is influence by the solutes. These results lead to a general description of interactions of small molecules with membranes helpful in understanding drug delivery across biomembranes and the mechanism of anesthetic action.

PROTEIN FOLDING

W-PM-Sym-1

THERMODYNAMICS OF PROTEIN CONDENSATIONS.
Gregorio Weber, School of Chemical Sciences, U. of Illinois.
The processes of protein subunit association and polypeptide folding (Protein condensations) are both driven by the excess entropy of the products. Contrary to a long-standing impression the changes in enthalpy and entropy with temperature are not fixed by the second law of thermodynamics but require specific thermodynamic models for their separation. One such model is that both enthalpy and entropy changes depend simply on the probability of thermal bond breaking. The free energy changes of the association of dimers and tetramers with pressure and temperature have been derived from that model and permit some general conclusions: 1: Entropy-driven reactions are only possible when the enthalpy changes of reactants and products virtually compensate each other so that $\sigma \approx 2\ \Delta H / (H_{pro.} + H_{react}) < < 1$. 2: A sufficient entropy change indispensably requires many bonds of energy less than 2 kcal/mol in the products and greater than 4 kcal/mol in the reactants. 3: The entropy increase on association depends upon conversion of the stronger protein-water (P-W) bonds into much weaker protein-protein (P-P) bonds. The conversion of P-W (hydrophobic bonds) into water-water bonds makes an insignificant contribution to the entropy change. 4: The dissociation of oligomers by hydrostatic pressure is due to the preferential destabilization by compression (Born repulsion) of the weak apolar bonds in the protein. 5: In several dimers and tetramers the enthalpy of association is approximately 25±5 kcal/mol per 1000 Å of contact surface. 6: Appreciable contributions to the entropy are limited to those bonds with breaking correlation times of less then 0.5 ns. Computations of protein folding alomg similar lines require further hypotheses concerning the relations of the entropy-driven apolar interactions and those owing to peptide dipole interactions.

W-PM-Sym-2

THE BARRIERS IN PROTEIN FOLDING. ((T. R. Sosnick, L. Mayne, S. W. Englander)) The Johnson Foundation, Department of Biochemistry and Biophysics, University of Pennsylvania, Philadelphia, PA 19104-6059.

Cytochrome c can fold rapidly, ~10 msec at 10° C, in a 2-state manner without populating intermediates. This establishes that all the required intrinsic steps in folding, including side-chain packing are inherently fast processes. These results are contrary to the current paradigm that particular steps in protein folding, including the supposedly rate-limiting molten globule to native transition, are intrinsically slow. It appears that kinetic intermediates so far characterized are trapped by barriers representing correction of misfolds formed in the initial collapse. When misfolding does not occur, our results with cyt c show that the intrinsic rate limiting step in folding is the initial collapse. Further experiments indicate that collapse is a nucleation process, limited by an energetically uphill conformational search for a relatively large scale configuration that can nucleate subsequent energetically downhill folding, perhaps through a defined sequence of intermediates, that leads to the native state.

W-PM-Sym-3

PROTEIN STRUCTURE PREDICTION BY MIMICKING FOLDING PATHWAYS. ((J. Moult)) Center for Advanced Research for Biotechnology.

W-PM-Sym-4

LINUS – A HIERARCHIC APPROACH TO PROTEIN STRUCTURE PREDICTION. ((George D. Rose and Rajgopal Srinivasan)) Johns Hopkins University, School of Medicine, Department of Biophysics and Biophysical Chemistry, 725 N. Wolfe Street, Baltimore, MD 21205. LINUS is a hierarchic procedure to predict the fold of a protein from its amino acid sequence alone. The name is an acronym for Local Independently Nucleated Units of Structure. The algorithm, which has been implemented in a computer program, ascends the folding hierarchy in discrete stages, with concomitant accretion of structure at each step. The chain is represented by simplified geometry and folds under the influence of a primitive energy function. The only accurately described energetic quantity in this work is hard sphere repulsion – the principal force involved in organizing protein conformation. Initially, LINUS was applied to large, overlapping fragments from a diverse test set of X-ray elucidated proteins, with generally accurate but rather imprecise prediction of overall fragment topology, including both secondary and supersecondary structure. Recent improvements to the program will be described.